AD-A037 238 RAYTHEON CO WALTHAM MASS RESEARCH DIV F/G 9/5
MANUFACTURING METHODS AND TECHNOLOGY MEASURES FOR ARC-PLASMA-SP--ETC(U)
JAN 77 H J VAN HOOK, D MASSE, J SAUNDERS DAAB07-75-C-0043
UNCLASSIFIED S-2156 NL

1 OF 2
AD A037238

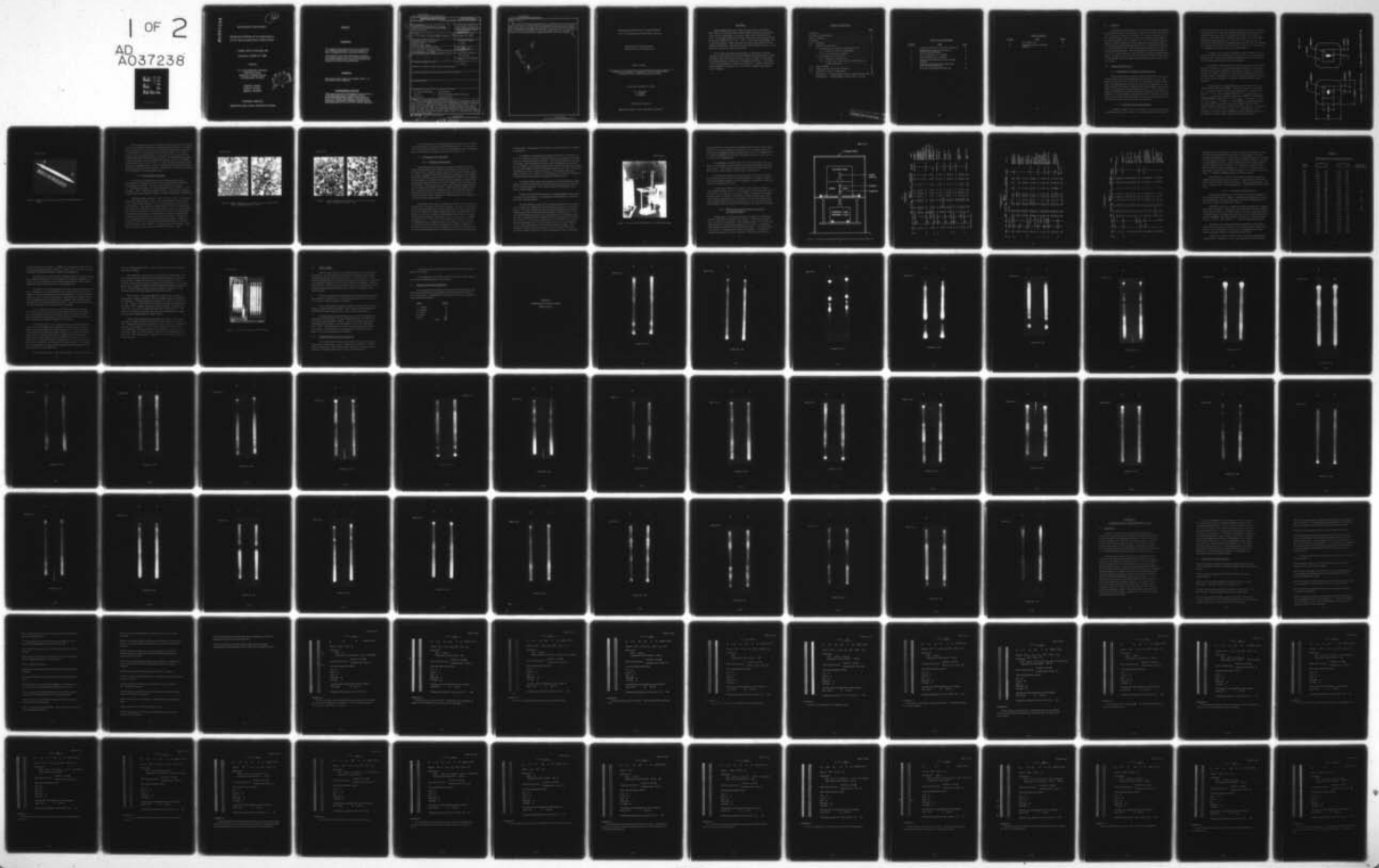

12

B.S.

Sixth Quarterly Progress Report

Manufacturing Methods and Technology Measure For Arc-Plasma-Sprayed Phase-Shifter Elements

1 October 1976 to 31 December 1976

Contract No. DAAB07-75-C-0043

Placed by

U. S. Army Electronics Command
Production Division
Production Integrated Branch
Fort Monmouth, NJ 07703

Raytheon Company
Research Division
Waltham, MA 02154

Distribution Statement

Approved for public release; distribution unlimited

NOTICES

Disclaimers

The findings in this report are not to be considered as an official Department of the Army position, unless so designated by other authorized documents.

The citation of trade names and names of manufacturers in this report is not to be construed as official Government indorsement or approval of commercial products or services referenced herein.

Disposition

Destroy this report when it is no longer needed. Do not return it to the originator.

Acknowledgement Statement

"This project has been accomplished as part of the U.S. Army (Manufacturing and Technology) (Advance Production Engineering) Program, which has as its objective the timely establishment of manufacturing processes, techniques or equipment to insure the efficient production of current or future defense programs."

Unclassified

SECURITY CLASSIFICATION OF THIS PAGE (When Data Entered)

REPORT DOCUMENTATION PAGE

READ INSTRUCTIONS BEFORE COMPLETING FORM

1. REPORT NUMBER

2. GOVT ACCESSION NO.

3. RECIPIENT'S CATALOG NUMBER

4. TITLE (and Subtitle)
Manufacturing Methods and Technology Measure for Arc-Plasma-Sprayed Phase-Shifter Elements

5. TYPE OF REPORT & PERIOD COVERED
Sixth Quarterly Progress
1 Oct. 1976 to 31 Dec. 1976

6. PERFORMING ORG. REPORT NUMBER
S-2156

7. AUTHOR(s)
H. J. Van Hook, D. Masse, and J. Saunders

8. CONTRACT OR GRANT NUMBER(s)
DAAB07-75-C-0043

9. PERFORMING ORGANIZATION NAME AND ADDRESS
Raytheon Research Division
28 Seyon Street
Waltham, MA 02154

10. PROGRAM ELEMENT, PROJECT, TASK AREA & WORK UNIT NUMBERS
2759441

11. CONTROLLING OFFICE NAME AND ADDRESS
U.S. Army Electronics Command
Production Div., Production Integration Branch
Fort Monmouth, NJ 07703

12. REPORT DATE
January 1977

13. NUMBER OF PAGES
111

14. MONITORING AGENCY NAME & ADDRESS (if different from Controlling Office)
Quarterly progress rept. no. 6, 1 Oct – 31 Dec 76

15. SECURITY CLASS. (of this report)
Unclassified

15a. DECLASSIFICATION/DOWNGRADING SCHEDULE

16. DISTRIBUTION STATEMENT (of this Report)
106p.

Approved for public release; distribution unlimited

17. DISTRIBUTION STATEMENT (of the abstract entered in Block 20, if different from Report)

18. SUPPLEMENTARY NOTES

19. KEY WORDS (Continue on reverse side if necessary and identify by block number)

Arc plasma spraying	Phase shifters
Ferrites	Microwave phase shifter materials
Dielectrics	Lithium ferrites

20. ABSTRACT (Continue on reverse side if necessary and identify by block number)

Seventy-eight plasma spray runs were made during this quarter. Half of these (39) were machined to phase-shifter dimensions and annealed before and after machining. Microwave testing was completed on 10 of these. For samples produced in the latter part of the quarter typical values of microwave phase shift are 370° - 420°, a considerable improvement over the previous quarter (~300°) and above the contract specifications of 340° saturation phase shift. Insertion loss in these phase shifters is 0.6 - 1.5 dB within the range of the contract goal (1 dB).

DD FORM 1 JAN 73 1473 EDITION OF 1 NOV 65 IS OBSOLETE

Unclassified

SECURITY CLASSIFICATION OF THIS PAGE (When Data Entered)

approximately

298 320

Abstract (Cont'd.)

We attribute the improved performance to refinements in vendor machining to give uniform ferrite wall thickness and improvements in spray techniques which have reduced cracking, and the avoidance of distortions during spraying due to temperature and alignment problems. Development of an X-ray fluoroscopic technique for nondestructive sample analysis has been invaluable in sorting out the courses of poor magnetic properties in earlier samples.

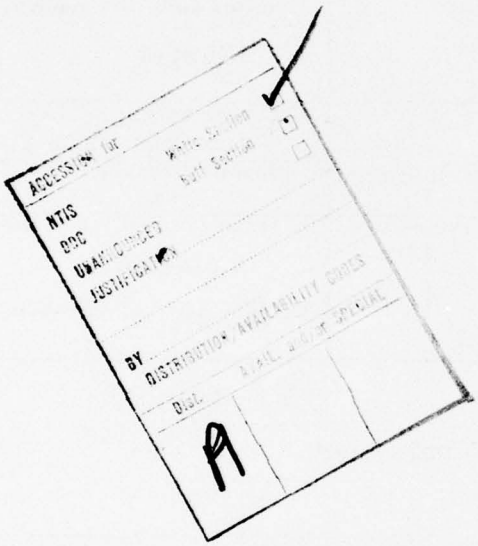

Manufacturing Methods and Technology Measure For Arc-Plasma-Sprayed Phase-Shifter Elements

Sixth Quarterly Progress Report
1 October 1976 to 31 December 1976

Object of Study

"The objective of this manufacturing and methods technology measure is to establish the technology and capability to fabricate phase-shifter elements by the arc-plasma spraying techniques."

Contract No. DAAB07-75-C-0043

H. J. Van Hook
D. Masse
J. Saunders

Distribution Statement

Approved for public release; distribution unlimited

ABSTRACT

Seventy-eight plasma spray runs were made during this quarter. Half of these (39) were machined to phase-shifter dimensions and annealed before and after machining. Microwave testing was completed on 10 of these. For samples produced in the latter part of the quarter typical values of microwave phase shift are 370° - 420°, a considerable improvement over the previous quarter (~ 300°) and above the contract specifications of 340° saturation phase shift. Insertion loss in these phase shifters is 0.6 - 1.5 dB within the range of the contract goal (1 dB).

We attribute the improved performance to refinements in vendor machining to give uniform ferrite wall thickness and improvements in spray techniques which have reduced cracking, and the avoidance of distortions during spraying due to temperature and alignment problems. Development of an X-ray fluoroscopic technique for nondestructive sample analysis has been invaluable in sorting out the causes of poor magnetic properties in earlier samples.

TABLE OF CONTENTS

LIST OF ILLUSTRATIONS

LIST OF TABLES

1.0 PURPOSE

The purpose of this program is to develop a manufacturing capability for producing the Patriot phase shifter element by arc-plasma spraying of a Li-Ti-ferrite onto a dielectric substrate. The primary objective is to produce the phase control element as a finished composition with acceptable microwave properties and a reasonably high yield. To achieve sound composites, one of the properties needing constant monitoring is the match in thermal expansion coefficient between the ferrite coating and the dielectric. A second important area for control and reproducibility is the thermal environment during spraying. Thermal conditions are influenced mainly by arc current, the gas velocities, and the substrate-to-gun separation distance. Finally, to achieve a low unit cost, it is necessary to improve yield and reduce machining costs by working with local machine shops to improve overall efficiency.

2.0 NARRATIVE AND DATA

2.1 Preparation and Testing of Starting Materials

During this quarter, attempts to optimize properties led us to use, in most spray runs, higher magnetization ferrite powder ($4\pi M_s$ = 1230 gauss) and two dielectrics very similar in composition and thermal expansion. By employing specific dielectric and ferrite compositions, we can also standardize conditions to help solve a serious problem in phase shifter yield. The problem, discovered during this quarter, is the distortion, or bowing, of samples during high-temperature processing. Such distortion appears to arise from spray techniques and rotation-translation equipment. These factors will be discussed in later sections, after properties of the fired dielectrics and the ferrite powder are described.

2.1.1 Dielectric materials development

A number of large (1 kg) bars of dielectric were fired and machined into substrates for the APS process. In earlier orders the broad cross-

sectional dimension of the center slot ran across the join of the two dielectric halves (Fig. 1a). Now all machining orders specify that the broad dimension of the center slot lie in the plane of the join of the two halves (Fig. 1b). There were three reasons for this change: (1) less breakage during handling and spraying due to the thicker cross section, (2) less interference with microwave propagation because length of the slot parallels the maximum microwave E-field at the center cavity, and (3) less problem in threading wires if the two halves are slightly offset.

Of course, we try to avoid any offset between the dielectric halves because it results in local thinning of the ferrite wall, which decreases B_r and phase shift. Offset also provides discontinuity in which cracks in the ferrite can propagate along the length of the phaser.

Fortunately, the stainless steel clips that we push on the ends of the dielectric (A and A' in Fig. 2) generally prevent offset of the two halves. However, the two halves separate or bow apart by .005 in. in the center region of the sample. Apparently, the force of the plasma spray spreads the pieces apart. Although we can reduce the problem somewhat by moving the clips in as far as possible, it cannot be eliminated with the present geometry.

The two dielectric compositions used primarily this quarter were LMTAF 200(7A) and LMTAF 200(4). Both have the same Li-Ti content ($x = 1.0$), but the former has less Al_2O_3 substitution ($w = 0.07$) than the latter ($w = 0.15$). The composition formula is $Li_{.5+x/2}Mn_{.10}Ti_xAl_wFe_{2.4-3x/2-w}O_4$ and the expansion coefficient at 1000°C (from the Fifth Quarterly Report, Table I) for $w = 0.07$, $\bar{\alpha}_{1000°} = 15.2$ ppm/°C and for $w = 0.15$, $\bar{\alpha}_{1000°} = 15.0$ ppm/°C. Other dielectric compositions used in the earlier part of this quarter were LMTF 200(2), LMTAF 190(15A), LMTAF 180(33), and LMTAF 195(10A), where the values of $\bar{\alpha}$ respectively are 15.4, 14.7, 14.7, and 15.0 in ppm/°C. There appears to be no systematic trend between the composition and the expansion coefficient of the dielectric and the magnetic properties of the phase shifters.

PBN-76-530

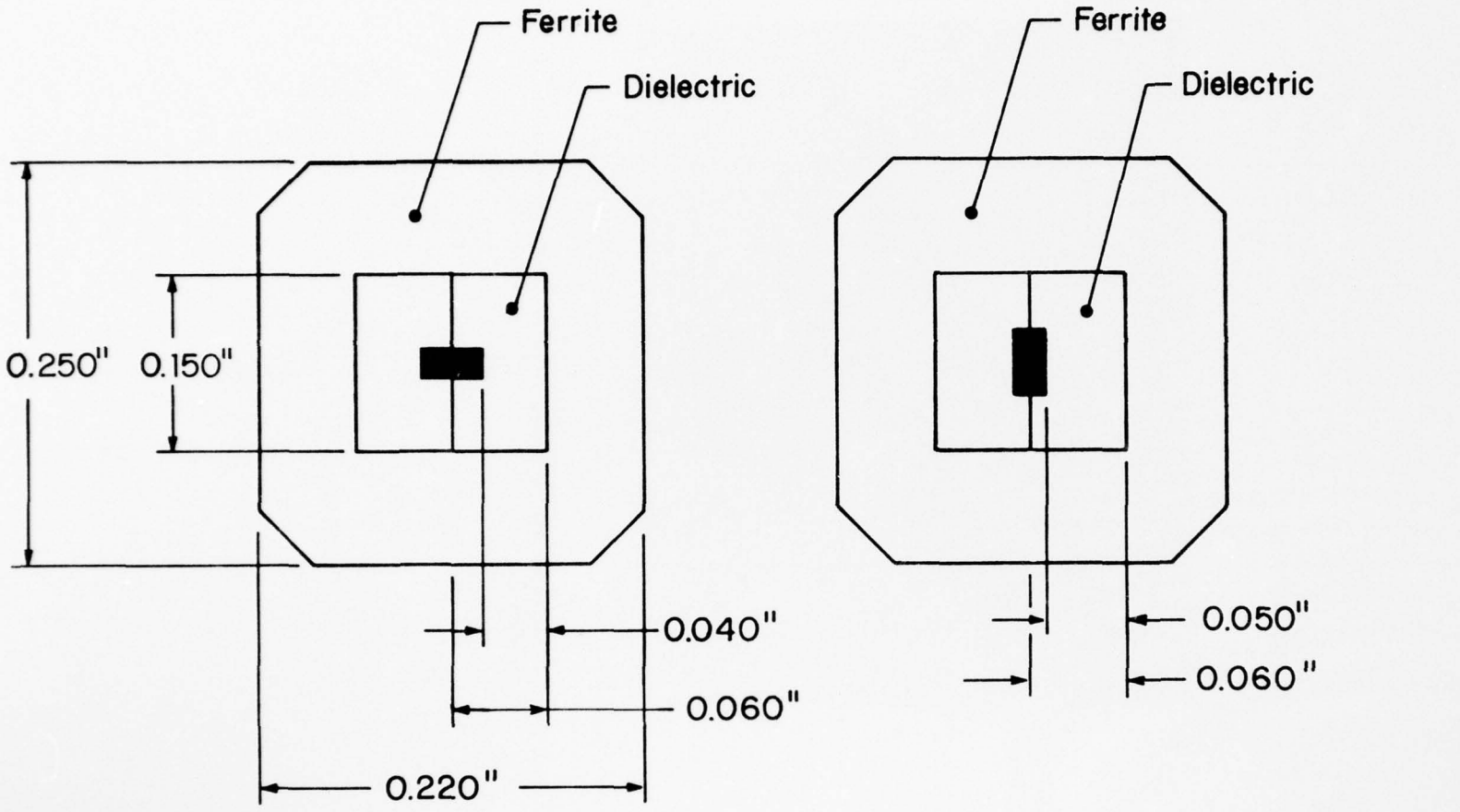

1a. Present 0.020"×0.040" slot

1b. New location of 0.020" × 0.040" slot

Figure 1 Location of the Slot in Two-Piece Dielectric.

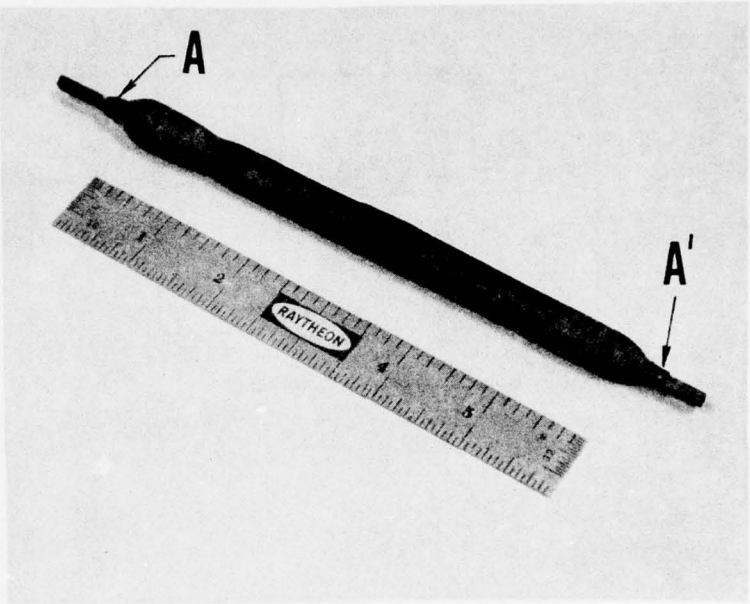

Figure 2 Stainless Steel Clips on the Ends of a Plasma-Sprayed Sample.

Our current main concern is maximizing yield of the dielectric pieces per bar, maintaining a fine-grained homogeneous microstructure for strength. The best yield to date is 35 dielectric pairs per bar, using about 32 percent of the original bar. Considering saw kerf losses (0.020 in.) and final reduction to size by grinding (0.010), we could expect a yield no greater than 45 percent for such small cross-section pieces. An additional material loss of about 30 percent occurs in the final phase shifter as we crop the length of the dielectric from ~7.5 in. to 5.145 in. Thus, the ultimate yield of a useful dielectric is about 22 percent. This is comparable to the present yield from the original spray-dried ferrite powder, starting from the initial ferrite powder and proceeding to the finished phase shifter.

2.1.2 Ferrite powder evaluation

The two ferrite powders used for APS runs this quarter were LMTF 50(G-4) for about one-third of the 80 runs and LMTF 475(G-5) for the remainder of the runs. The former has a higher Li-Ti content ($x = 0.50$) and lower $4\pi M_s$ (~1175 gauss) than the G-5, in which $x = 0.475$ and $4\pi M_s = 1230$. When conventionally fired ($d_x > 99$ percent), the magnetization of both ferrite powders is higher (~1250 and 1330 gauss, respectively).

SEM photographs originally at 400× for the G-4 and G-5 spray-dried powders are shown in Figs. 3 and 4. The sprayed powder collects either in the original settling chamber or in the cyclone separator located on the air exhaust line. The spray-dried balls of powder from the chambers have larger diameters than most of the balls of powder from the air exhaust line, which is carried further in the hot gas stream. However, the photographs clearly show a much wider size distribution in the fines fraction because "chambers size" particles are carried by the gas stream. Although the size distribution has not been analyzed by particle counting, it appears to be similar to the G-3 ferrite powder processed identically (see the Third Quarterly Report, Figs. 6 and 7). Average diameter for G-3 powder in the fines fraction was ~5μm and for the chambers fraction, ~8μm.

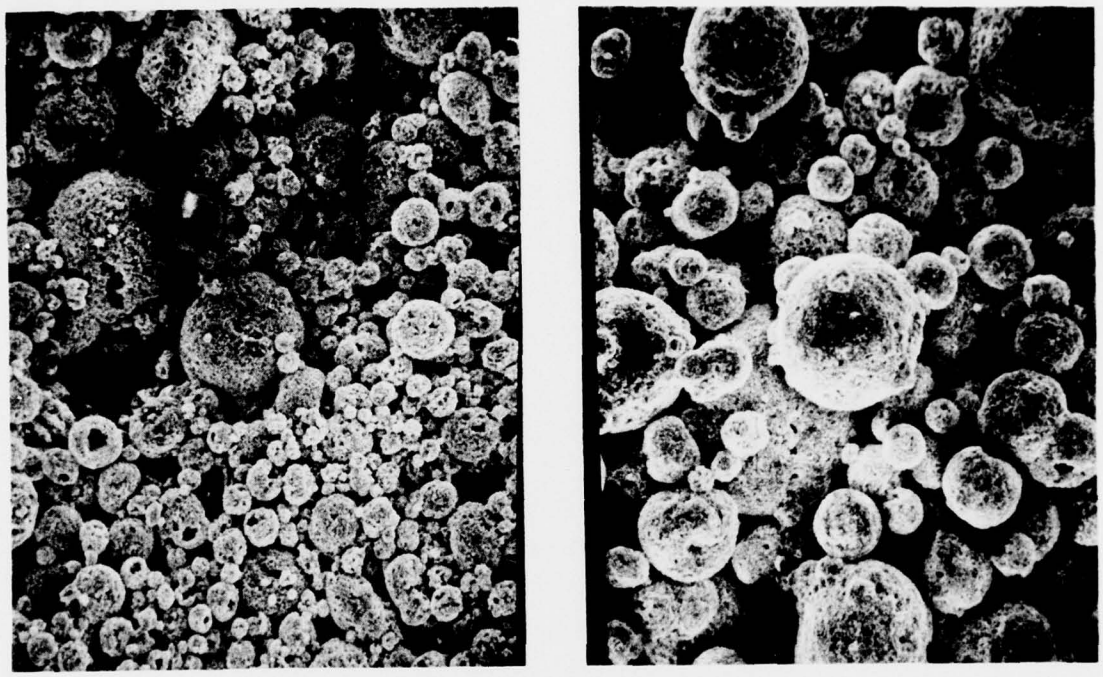

Figure 3 SEM Photograph of G-4 Powder. Left: Fines Fraction. Right: Chambers Fraction. ×295

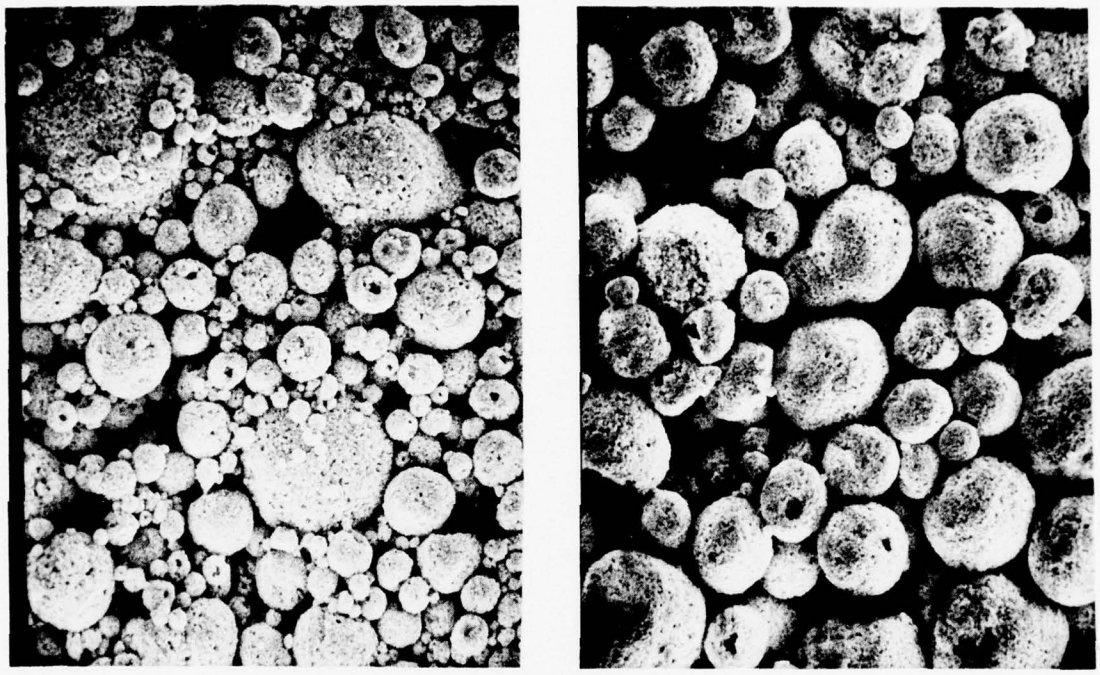

Figure 4 SEM Photograph of G-5 Powder. Left: Fines Fraction. Right: Chambers Fraction. ×295

In the APS process we have found empirically that screening through a 170-mesh (88-μm) sieve gives a smooth-flowing powder. One can see that very few particles exceed 88 μm: the screening probably breaks up aggregates rather than separating any significant number of big particles.

2.2 APS Experiments at Raytheon

2.2.1 Equipment modifications

The plasma spray holding furnace and spray chamber were used without modification in basic configurations during this last quarter. With the change from a cylindrical spray chamber at the end of the fourth quarter to a longer rectangular oven we had reduced the turbulence of the overspray powder and problems arising from buildup on furnace walls. The amount of electrical power in the larger chamber has been adequate to maintain 700°C during spraying but the recovery time after sample transfer is slower than we would like. During spraying, the heat from the plasma supplements the electrical heating, but during transfer, temperature drops approximately 100°C from heat transfer to the pedestal tube. The latest plan calls for more heating elements and an additional volume increase in the spray chamber to further reduce turbulence of spent powder and the temperature excursions during sample transfer.

On October 30 the contract called for the delivery of 20 confirmatory samples before moving into the production phase. We found, unfortunately, that almost all the phase shifters intended for delivery were approximately 20 percent deficient in remanent magnetization (B_r) and phase shift. Initially we could find no consistent relationship between dielectric composition and spray conditions, on one hand, and B_r, on the other, to explain our observations. It was not until we performed sectioning and, later, X-radiography that we found the cause of the problem: Non-uniform ferrite walls produced by warping and bowing of the sample, apparently during the spray process, since the dielectric is machined straight before processing and the sprayed boule is machined to exact external dimensions

after spraying. Photographs of all of these low-B_r phase shifters are shown in Appendix B.

By applying X-radiography as a quality-control tool, we believe that one of the contributing factors to sample distortion is the imperfect functioning of the rotation-translation equipment. By careful measurement we found, for example, that the position of the top end of the pedestal tubes varied as much as 0.200 in. in the horizontal plane with successive up and down cycling. The top of the substrate, which extends approximately 7 in. above the pedestal, would show even more variation in position. With a plasma spray cone approximately 0.5 in. in diameter at the deposition site, any such irregularity in position would clearly cause an asymmetric deposit pattern.

We theorized that radial nonuniformities in the deposit pattern would produce differential temperatures and differential strains, which could produce the warping observed. This situation could be controlled by a more exactly aligned system.

Earlier work at ECOM Laboratories yielded good phase shifters with irregular rotation. However, the equipment in our laboratory is different, and so are the requirements.

We have rebuilt the rotation and translation equipment in our laboratory to improve the reliability of sample translation relative to the present system. It will be installed after the confirmatory samples are delivered. A photograph of the new pedestal tubes assembly is shown in Fig. 5. The tube and rotational drive motor move up and down on the rectangular block (b), which is guided by linear bearings within the block and the two vertical guide rods (g). The end of the pedestal tube (p) is made to rotate on axis by screw adjustments on two metal disks at the base of the tube having a 0.5 in. steel ball captured in retaining slots between the disks. This pedestal assembly, which has leveling screws at the base, will sit on a steel plate, which is attached to metal rods suspended from a metal plate.

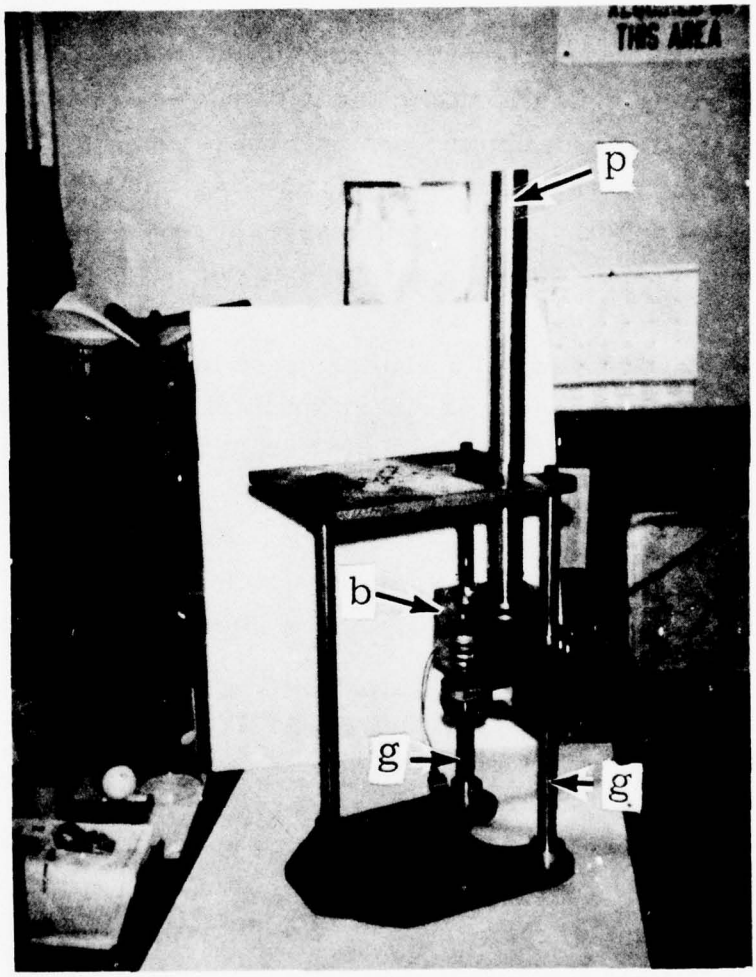

Figure 5 Pedestal Tube Assembly for Arc-Plasma Spraying.

This metal plate, in turn, underlies the plasma spray furnace and the upper holding oven. Such an elaborate arrangement of metal support plates and interconnected equipment (shown schematically in Fig. 6) is designed so that the pedestal assembly (ped) and spray and holding ovens are interconnected and cannot move independently.

Very possibly, the substrate may still wobble at the free end. If it does, we will introduce an upper idler bearing (see dashed lines) to capture the free end. In this scheme a graphite part replaces the upper metal clip and provides a conical tip for rotation within the bearing tube.

This bearing assembly was built and tested on November 22 (APS 252-256) with our own original translation equipment. Alignment, however, was simply not good enough, and all the substrates except for APS 252 were broken by misalignment stresses.

We hope that it will not be necessary to use the upper bearing to avoid substrate wobble, that is, that the improved pedestal assembly (Fig. 5) will be sufficient. However, we are proceeding to interconnect the supporting plates (Fig. 6), so that, if necessary, the upper bearing can be used. Our objection to the bearing is that it would have to be removed after each run for sample transfer into the holding oven. We have arranged for exact repositioning, but the bearing would be hot (600°C) and difficult to maneuver.

2.2.2 Plasma spray runs and hysteresis properties on machined samples

Plasma Spray runs 218 through 296 were completed in this quarter. The APS conditions are summarized in Table I . Hysteresis data were taken on many of these samples. APS samples from 137 to 239 (those originally intended for confirmatory samples) were X-rayed to evaluate the contributions of cracks and wall nonuniformities to B_r. The results of this study and the X-radiographs are included in Appendix A. Samples 239 through 256 represent a transition period, in which tests were made to

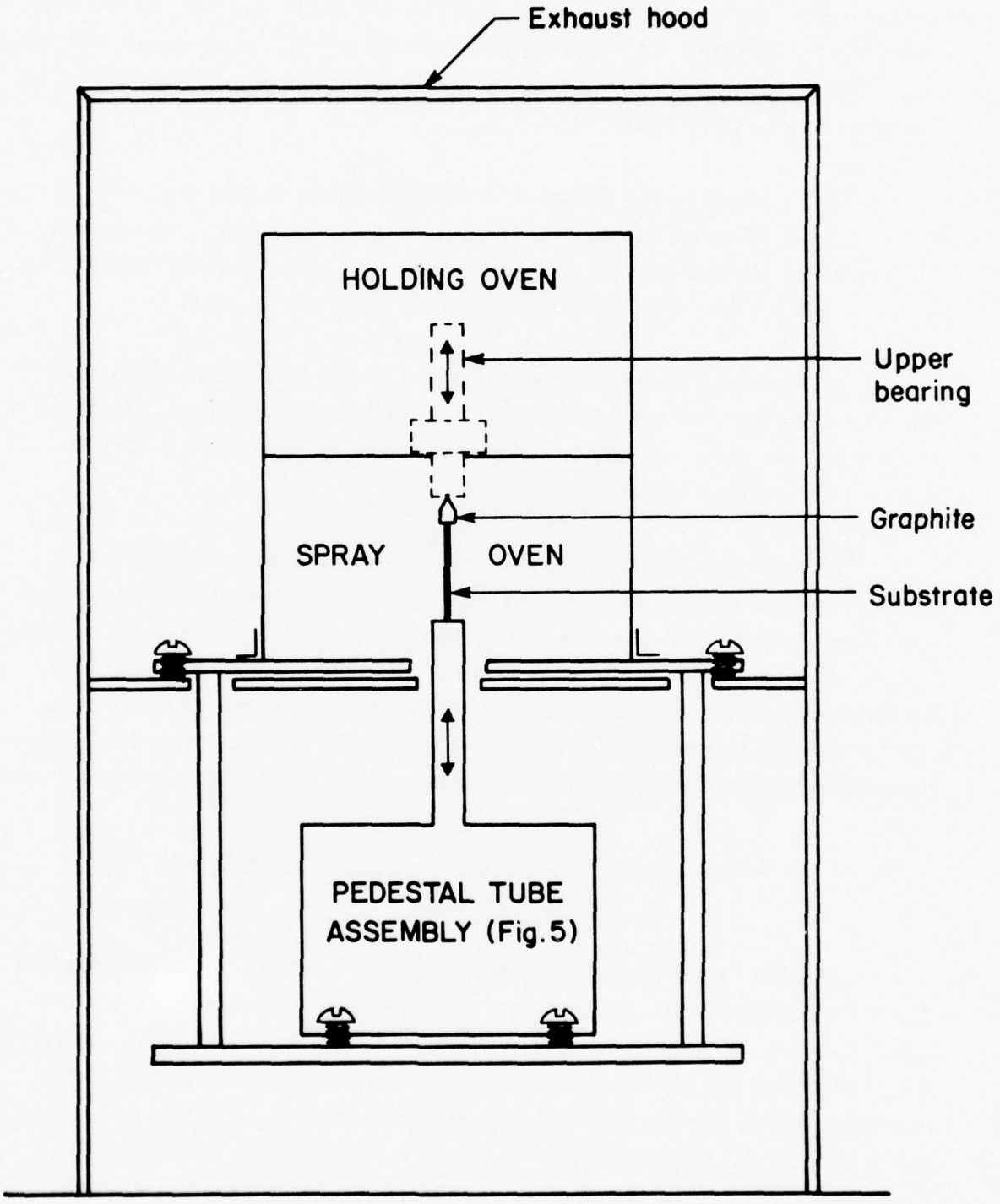

Figure 6 Diagram of Metal Supporting Plates and Interconnected Equipment

TABLE I

ARC PLASMA SPRAY LOG
High Velocity Nozzle

Date	Number	Ferrite	Dielectric	Current Amps	Gas Flow - CFH Arc	Gas Flow - CFH Powder	Hopper Speed %	Spray Distance in	Spray Distance Rot %	Rate Pull in/min	Furnace Temperature Chamber	Furnace Temperature Holding	Anneal Cycle*	Comment
10/6	218	LMTF475G-5 -88μ*	LMTAF190-15A	300	Ar 38	O_2 15	65	3 1/4	50	0.6	700	650	1020°(H)-2Hrs. O_2	Anneal conditions not recorded
	219	↓	↓	400	Ar 38	O_2 14	65	3 1/4	50	1.2	↓	↓	↓	Air in hydraulic line causing poor start
	220			320-420	Ar 38	O_2 14	65-75	3 1/4	45	1.0				Current fluctuating as much as 100 amps
	221			420	Ar 45	O_2 14	65	3 1/4	45	1.1				Wobble forced slower rotation rate
	222			420	Ar 45	O_2 14	65	3 1/4	45	1.1				Higher velocity affects sample rotation and eccentricity
10/11	223	LMTF475G-5 -88μ	LMTAF190-15A	440-450-460	Ar 38	O_2 13	70	3 1/4	50	0.6	710	650	1016°(11)-3Hrs. O_2	Substrate large grained - left in furnace during previous anneal
	224		LMTAF180(33)	450-340	Ar 38	O_2 25	65	3 1/4	45	0.6	710	685		New anode and cathode for this day's run - flame firing upward - needed more powder gas
	225		↓	320-400	Ar 38	O_2 25	70	3 1/4	42	.6-.8	710	680		
10/12	226	LMTF475G-5 -88μ	LMTAF180(33)	360	Ar 38	O_2 25	65	3 1/4	50	0.8	700	-0-	1050°-O_2	Quick anneal - no soak - broke apart - cathode check
10/13	227	LMTF475G-5 -88μ	LMTAF190-15A	320	Ar 40	O_2 30	65	3 1/2	42	0.6	700	650	1000°(11)-5Hrs-O_2	Sample fell in dismount
	228	↓	↓	380	Ar 40	O_2 17	65-70	3 1/2	50	1-0.6	675	650	↓	Seal leak at hopper
	229			380	Ar 40	O_2 17	70	3 1/2	50	1-0.6	675	650		
	230			380	Aborted - Element Failed									
	231	LMTF475G-5 -88μ	LMTAF200(2)	350	Ar 40	O_2 15	65	3 1/4	50	0.6	700	650	1000°(11)-5Hrs-O_2	Power buildup - broke two substrates
	232	↓	↓	320	Ar 40	O_2 15	50-40	3 1/4	50	0.6	700	650	↓	
	233			320	Ar 40	O_2 15	50	3 1/4	50	0.6	700	650		Left TC malfunctioning
10/14	234	LMTF475G-5 -88μ	LMTAF200(2)	380-400	Ar 40	O_2 20	35	3 1/4	50	0.7	620	650	1000°(11)5Hrs-O_2	Left TC failed
10/15	235	LMTF475G-5 -88μ	LMTAF195-10A	350	Ar 40	O_2 12	65	3 1/4	50	0.8	750	650		
	236	↓	↓	360	Ar 38	O_2 13-18-22	65	3 1/4	50	0.8	750	650	1000°(11)5Hrs-O_2	
	237			330	Ar 38	O_2 22	65	3 1/4	50	0.8	736	650	↓	Pull rate system will not hold set rate - continually decreases
	238		LMTAF190-15A	320	Ar 38	O_2 22	65	3 1/4	38	0.8	750	650		
	239		↓	365	Ar 38	O_2 23	65	3 1/4	38	0.9-1.0	645	650		
10/22	240	LMTF50G-4 -88μ	LMTAF195-10A	320	Ar 38	O_2 17-22	65-75	3 1/4	50	1.0	660	370		
	241	↓	↓	320	Ar 38	O_2 22	65	3 1/4	50	0.75	625	450	1016°(11)-2Hrs-O_2	Annealed in sand to avoid distortion
	242			320	Ar 38	O_2 22	65	3 1/4	50	0.95-.8	690	483	↓	

* Screened through 170 mesh (88μ)

ARC PLASMA SPRAY LOG (Cont'd.)
High Velocity Nozzle

Date	Number	Ferrite	Dielectric	Current Amps	Gas Flow - CFH Arc	Gas Flow - CFH Powder	Hopper Speed %	Spray Distance in	Rot %	Rate Pull in/min	Furnace Temperature Chamber	Furnace Temperature Holding	Anneal Cycle*	Comment
10/22	243	LMTF475G-5 -88μ	LMTF 200(2)		Dielectric Broke									
	244	↓	LMTAF 195-10A	320	Ar 38	O_2 22-28	65-75	3 1/4	42	0.8	645	450		Sample dropped ~ 1/2 in. during spray - overlap
10/26	245	LMTF50G-4 -88μ	LMTAF 195-10A	360	Ar 38	O_2 25	75	3 1/4	50	0.8-0.9	685	485	No Anneal	Ammeter of hopper @ 210 (420) milliamps
	246			320	Ar 38	O_2 25		Sheared Off				560		
	247			320	Ar 38	O_2 25	65	3 1/4	40	1.0	700	650		Jaws appeared to loosen after 1 in. of spraying
	248	LMTF475G-5 -88μ		320	Ar 38	O_2 15	65	3 1/4	50	1.0	685	650		Substrate wobbly - finally broke
	249			320	Ar 38	O_2 15-21	65	3 1/4	40	1.0	700	672		G-5 Powder flowed better than G-4
	250			320	Ar 38	O_2 22	65	3 1/4	42	0.9	700	650		
	251			320	Ar 38	O_2 18	65-50	3 1/4	40	0.7	700	675		Too much wobble for all samples
11/22	252	LMTF50G-4 -88μ + 44μ	Fe_2O_3-Solid	400	Ar 40	O_2 30	65	3 1/4	40	1.0	525	350		First use of graphite Top keeper - unsuccessful
	253		LMTAF 200(4)	380	Ar 40	O_2 15-25	50-65	3 1/2	50	0.4-0.7	620	650	1015°(11)-2Hrs. -O_2	Poor deposit
	254			380	Ar 40	O_2 25-30	55	3 1/4	50	0.5-.65	635	650		Poor powder flow
	255			380	Ar 40	O_2 20-27	60	3 1/4	50	0.5	640	650		Broke in raising - "upper" spray
	256	Not Temp. Conditioned		420	Ar 40	O_2 30	80	3 1/4	50	0.8	700	650		Broke - half sprayed - good deposit - hit obstruction
12/6	257	LMTF50G-4 -88μ	LMTAF200(4)	350	Ar 40	O_2 20	65	3 1/4	50	0.8	660	650	1015°(11)-2Hrs. -O_2	New powder hose - not a good sample - warped
	258		LMTAF195-10A	350	Ar 40	O_2 20	65	3 1/4	50	0.8	675	650		Powder flow improved as spraying continued
	259			350	Ar 40	O_2 20	65	3 1/4	50	0.8	640	600		258, 259 "upper" spray - spitting and too much wobble
12/6	260	LMTF50G-4 -88μ	LMTAF195-10A	350	Ar 40	O_2 16	65	3 1/4	50	1.0	665	600	1015°(11)-2Hrs. -O_2	Blew gun out before spray
	261	↓	LMTAF200(4)	350	40	16	60	3 1/4	50	0.6	660	600		"Upper" spray - ran out of powder
12/9	262	LMTF475G-5 -88μ	LMTAF200(4)	360	40	15-30	65-50	3 1/4	50	0.5	700	720	1015°(11)-2Hrs. -O_2	Powder left in system did not spray well
	263			360	40	25	65	3 1/4	50	1.0	700	720		
	264			360	40	25	50-55	3 1/4	50	0.9	700	710		Sample broke, upper spray
	265			360	40	25	55	3 1/4	50	0.8	700	710	No Anneal	So much wobble that rot.
	266			300	40	25	60	3 1/4	50-30	0.8-0.6	700	725		rate just moving - broke in chamber - left to cool
12/13	267	LMTF475G-5 -88μ	LMTAF200(4)	220	35	13	60	2 7/8	50	0.8	700	600	Aborted because of substrate split	
	268			240	35	13	60	2 7/8	45	1.0	700	600	1015°(11)-2Hrs. -O_2	
	269			230	35	17-10	50-60	2 7/8	50	1.1	700	600		

ARC PLASMA SPRAY LOG (Cont'd.)
High Velocity Nozzle

Date	Number	Ferrite	Dielectric	Current Amps	Gas Flow - CFH Arc	Gas Flow - CFH Powder	Hopper Speed %	Spray Distance in	Rot %	Rate Pull in/min	Furnace Temperature Chamber	Furnace Temperature Holding	Anneal Cycle*	Comment
12/13	270	LMTF475G-5 -88μ	LMTAF200(4)	200	Ar 35	O_2 10	60	2 7/8	45	1.0	675	600	1015°(11)-2Hrs.-O_2	
	271			300-270	35	12	60	2 7/8	45	1.3	700	600	Aborted because of substrate split	Current too high
	272			250	35	11	60	2 7/8	45	1.3	700	600		
	273			220	35	11 1/2	60	2 7/8	45	1.1	685	600		
	274			210	35	12	60	2 7/8	45	1.1	700	700		
12/16	275	LMTF475G-5 -88μ	LMTAF200(4)	240	35	12	60	2 7/8	50	1.0	600	650	1015°(11)-2Hrs-O_2	Spray chamber a bit low in temperature
	276			210	35	17	50-60	2 7/8	50	1.0	690	600		
	277			210	35	12	60	2 7/8	Fwd 50	1.0	650	600		Wobble ~ 1/8 in.
	278			210	35	12	50	2 7/8	50	1.0	655	600		Wobble ~ 1/8 in. Broken near base
	279			210	35	12	50	2 7/8	Rev 45	1.0	690	600		
	280			210	35	12-10	50	2 7/8	50	0.8	675	600		Deposit thinned - "Upper" Spray
	281			210	35	10	40	2 7/8	45	1.0	680	700		
	282		Not Preheated (NP)	210	35	10	50	2 7/8	45	1.3	700	600		Substrate not preheated
	283			210	35	10	50	2 7/8	45	1.2	690	600		Ran out of powder
	284	LMTF475G-5 -88μ	LMTAF201-7A	210	35	10	50	2 7/8	50	1.0	700	600	1015°(11)-2Hrs-O_2	Substrate separation on initiating spray - a continuous problem
	285			210	35	10	F50R	2 7/8	50	1.0	700	600		
12/21	286	LMTF475G-5 -88μ	LMTAF201-7A	210	35	O_2 11	50	2 7/8	50	1.1	700	600	1015°(11)-2Hrs-O_2	3/16 in. wobble initially but improved with spraying - back vent brick(Lge) replaced to conserve chamber heat - jaw tension may have decreased - jerky rotation
	287			210	35	12	50	2 7/8	45	1.0	700	600		
	288			220	35	12	50-60	2 7/8	45	1.2	700	600		
	289			220	35	13	50		40	1.1	700	600		
	290			220	35	12	50		40	1.1	710	600		
	291			220	35	12	50-45		40-35	1.0	710	600		Blobs increasing - but near it good- no change made
	292			Broke after 1/2 in. deposit										
	293		NP	220	35	12-15	45-55		35	1.1-1.5	710	600		No preheat for substrate - (NP)
	294		NP	220	35	15	50		35	1.2	700	600		Current fluctuated briefly
	295		NP	220	35	15	45		35-30	1.1	700	600		Current initially at 200 - poor deposit
	296		NP	220	35	15	60		30	0.7	690	600		Short section for heavy deposit

identify the causes of substrate warping and during which an upper bearing assembly was built and tested in an effort to avoid warping. The upper bearing was generally unsuccessful because of alignment problems, and many dielectric rods were broken. In December we continued without the bearing assembly (APS 257 et seq.), using X-radiography to weed out the warped or cracked samples before machining. The radiographs of sprayed boules (APS 257-295) are shown in Appendix A. The letter H indicates that the photograph was taken in a direction perpendicular to the join of the dielectric halves; V signifies a photograph taken parallel to the join.

Runs 262 et seq., made of the G-5 powder exclusively, provided samples that produced better phase shifters. Typical phase-shifter values in this series are 400°, which is well above $> 340^{\circ}$, the program goal. This was accomplished with a ferrite having $4\pi M_S = 1230$ gauss in plasma-sprayed form.

2.2.2.1 Description of individual runs

The spray run on October 6 (see Table II) was the first attempt to use the new spray-dried G-5 powder. Mechanical problems such as air in the hydraulic line, arc current fluctuations, and poor clamping by the pedestal jaws produced generally poor samples.

On October 11 and 12 we again tried spray runs with the G-5 powder and various substrates. In these two runs we had difficulty with the powder spray pattern, which was eventually traced to a defective anode and cathode. Two good samples were produced on October 11, one of which (APS 224) was broken in handling. The second sample, APS 225, was a good specimen, with $B_r = 715$, $\Delta\Phi = 365^{\circ}$, and I.L. = 1.1 dB (see confirmatory report).

On October 13 we again had mechanical difficulties with powder leaks in the feed hopper and, finally, heater element failure, which ended the run. The ferrite powder (G-5) was also clogging the nozzle of the plasma spray gun, despite screening and drying at $60^{\circ}C$.

On October 14 and 15 we had our first reasonably successful runs of this quarter. Spraying at 3.25 in., the deposit rate was rather slow

TABLE II

HYSTERESIS DATA ON APS RUNS 262-295

Sample No.	6 Amps Drive H_c	6 Amps Drive B_r	15 Amps Drive H_c	15 Amps Drive B_r	Phase Shift 15 Amps Drive
262	1.91	733	1.88	796	
263	2.41	630	2.57	706	
264	2.50	737	2.73	823	
268	1.67	178	2.89	696	
269	1.47	138	2.75	704	
270	1.89	319	2.36	754	
272	1.88	172	2.84	710	
273*	1.80	220	2.81	745	
274	1.84	201	2.67	751	380°
275	1.80	321	2.37	641	
276	1.70	248	2.32	725	
277	1.56	433	1.93	764	380°
279	1.76	150	2.83	782	416°
280	1.92	181	2.62	535	
281	1.93	274	2.63	795	410°
282	1.96	285	2.82	821	423°
284*	2.10	364	2.58	757	
286	1.96	467	2.39	771	
287	1.94	354	2.26	670	
288*	2.07	358	2.56	754	
289	2.09	337	2.69	792	
291	1.95	155	2.91	739	
293	1.81	134	2.99	748	
294	1.86	149	2.87	800	
295	2.44	274	2.84	726	

compared with later experience. In addition, we experienced some difficulty with thermocouple malfunction. However, samples 231, 234, 237, 238, and 239 produced relatively good phase shifters (see Appendix A).

By mid-October we had found the warping problem to be rather serious. After trying and rejecting several techniques for evaluating straightness, we finally chose X-radiography and began photographing finished phase shifters (Appendix B) and as-sprayed boules as well (Appendix A).

The October 22 run was planned to determine when the distortion takes place. Originally, we suspected that the bare dielectric rods were being deformed by a creep mechanism before the APS deposition. To reduce this possibility, we built a metal rig from which to suspend the rods before spraying. Also the holding oven was turned down to a minimal value ($\sim 400^{\circ}C$) during spraying and shut down immediately thereafter. The as-sprayed boules were X-rayed for straightness the next day before annealing.

The X-rays showed two of the three APS samples (241 and 242) were bowed, proving that at least some distortion takes place during spraying. We concluded that bowing is probably connected with uneven radial powder deposition during spraying, which likely occurs with uneven rotation of the pedestal and consequent wobbling of the substrate.

On November 22 we tried an upper-bearing assembly designed to reduce the free-end wobble of the substrates. A metal frame was rigidly attached to the bottom plate of the upper holding oven. A slot in the metal frame allowed us to repeatedly position a large (3-in. diameter) stainless steel bearing. A stainless tube slides vertically within the bearing and makes contact with a graphite part on the substrates (see Sec. 2.1.1). Unfortunately, we could not maintain the alignment of the pedestal, and dielectrics broke, usually near the completion of a spray session. We concluded that we could not use the upper bearing assembly until we significantly improved the lower pedestal alignment.

Of the samples APS 245 - 256, only APS 252, a one-piece dielectric,

survived spraying without failure. This sample broke up due to expansion mismatch on cooling.

The December 6 run made use of the LMTF 50(G-4) poweder, which we knew had good flow characteristics and eliminates problems connected with poor flow. Sample 257 was sprayed from the top down (our usual practice), whereas 258 and 259 were sprayed from the bottom up. The radiographs show extensive cracking in 258 and nonuniform longitudinal deposition in 259. Sample 260 had a necked area due to powder clogging in the gun. Deposition of APS 261 looked good until the powder ran out.

On December 9 we began using the G-5 powder, after additional drying and screening, producing a series of samples under fairly standardized conditions. Warping shows up in APS 262, 273, and 278, but the others are quite straight. Sample APS 280, sprayed by the nonconventional bottom up method, shows abundant cracks due to thermal shock. A photograph of some of the more recent samples (APS 284-296) is shown in Fig. 7. The samples are embedded in zirconia sand to avoid any possibility of warping due to gravity settling during the 1015^{o}C anneal.

Table II gives hysteresis data on APS runs 262-295. These data represent a change in measurement procedure from two to one turn of drive wire. Earlier hysteresis data reported as 6 and 15 amps drive actually had two turns, which means 12 amp-turns and 30 amp-turns. In this case a sample showing $> 340^{o}$ phase shift had a $B_r > 720$ gauss. For one-turn-drive phase shifters (see Table III) $B_r = 650$ gauss, corresponding to 340^{o} phase shift. The saturation phase shift for 5 of the 25 samples is given in the last column.

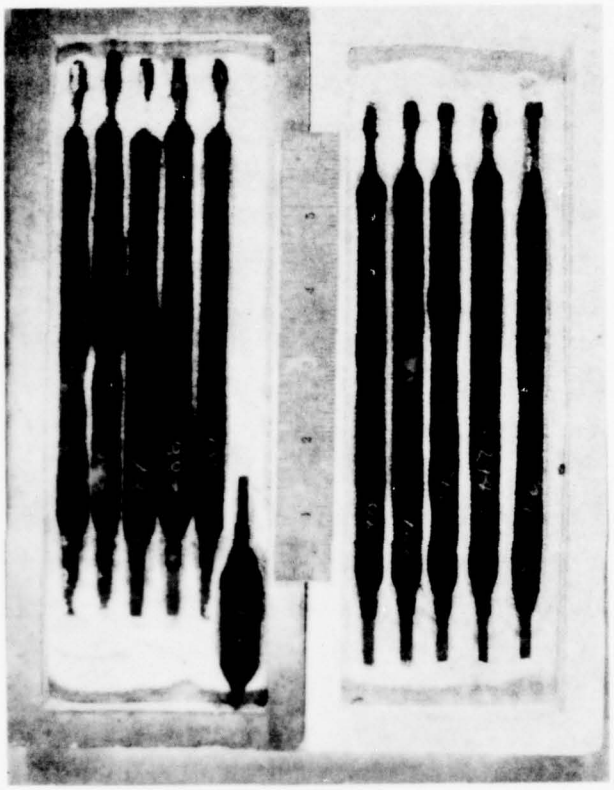

Figure 7 Some Recent Samples (APS 284-296).

3.0 CONCLUSIONS

There has been some very real progress made in the APS process this quarter. We have uncovered a major cause of the low B_r in samples originally intended for the confirmatory run. The original series of runs yielded 4 good samples out of more than 100 runs (39 of which were machined). The predominant reason for low yield was warping of the element during the spray process. Another contributing factor the G-4 a ferrite powder, whose saturation magnetization was slightly lower than the G-5 powder we subsequently used.

We have not identified and quantified all the factors producing warping. However, we know that an uneven radial coating of ferrite is a factor as is excessive spray temperature conditions.

We have developed a diagnostic technique to screen out cracked or deformed samples before machining. This technique will be invaluable in uncovering the spray conditions which lead to sample deformation.

In samples 262 through 296 (sprayed at the end of the quarter) the yield improved substantially. Of the 35 samples sprayed, 22 were made into full-size phase shifters (Table II), and 3 were bowed, necessitating machining in two sections. Of the 22 samples 19 have a B_r indicating $\Delta\Phi > 340°C$. The overall yield has been increased from about 4 percent to 54 percent. If this yield can be maintained in the production run to follow, the contractural goal will be satisfied.

4.0 PROGRAM FOR THE NEXT INTERVAL

The redesign and rebuilding of the rotation-translation equipment is underway at this writing. After the installation is complete, we plan a number of spray runs to determine whether reliability is improved and to reproduce the sample yields obtained at the end of this quarter.

We will then await permission to proceed with the final production phase of the contract.

We will also update the PERT chart for the entire contract interval to reflect the scheduling changes in this quarter.

5.0 IDENTIFICATION OF PERSONNEL

The personnel who contributed to this production development effort during the sixth quarterly reporting period, and the manhours worked by each is shown below. Biographies of these personnel have been supplied in previous quarterly reports.

Name	Hours
J. Van Hook	32
L. Lesensky	1
W. Griffin	18
R. Maher	56
Others	176
Total	283

Appendix A

X-Radiography of Plasma-Sprayed Boules 257-295

H V

PBN-77-61

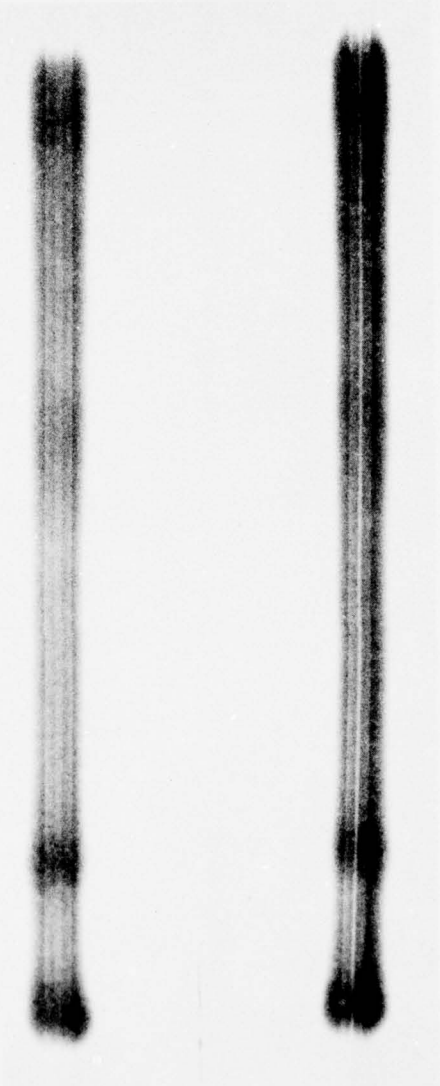

Sample No. 257

H V

PBN-77-62

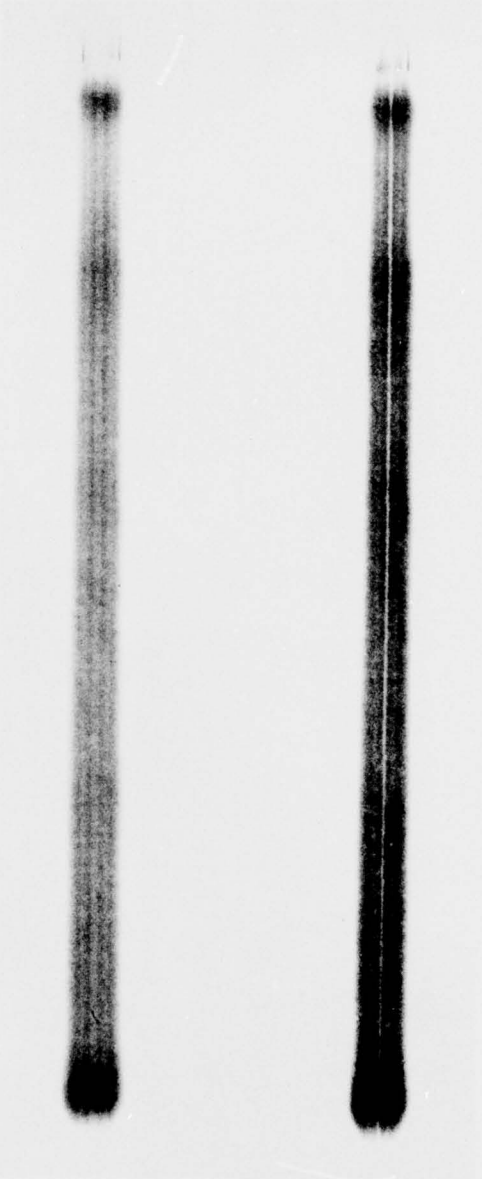

Sample No. 258

H V

PBN-77-63

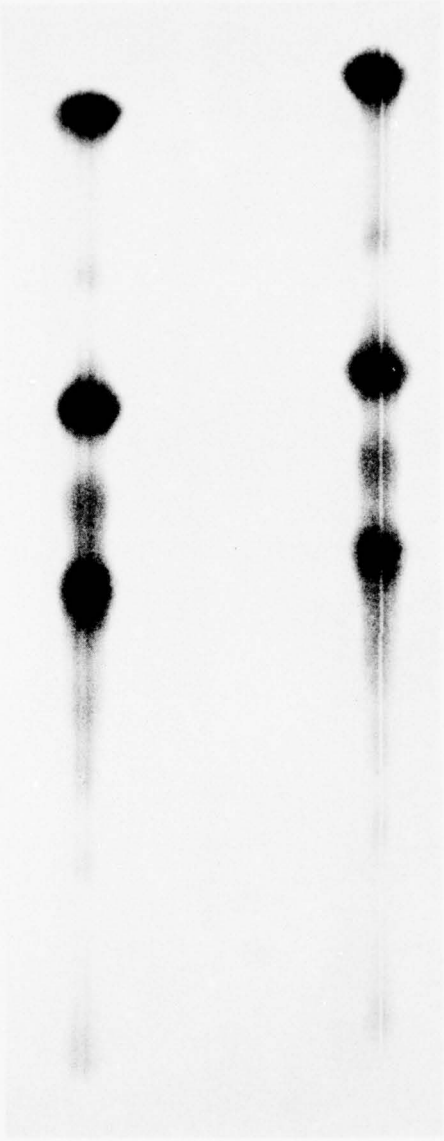

Sample No. 259

H V

PBN-77-64

Sample No. 260

H V

PBN-77-65

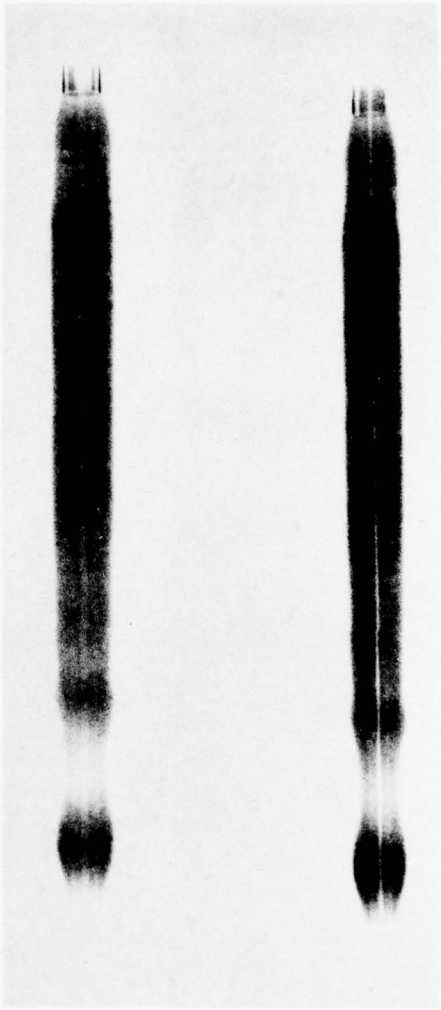

Sample No. 261

H V

PBN-77-67

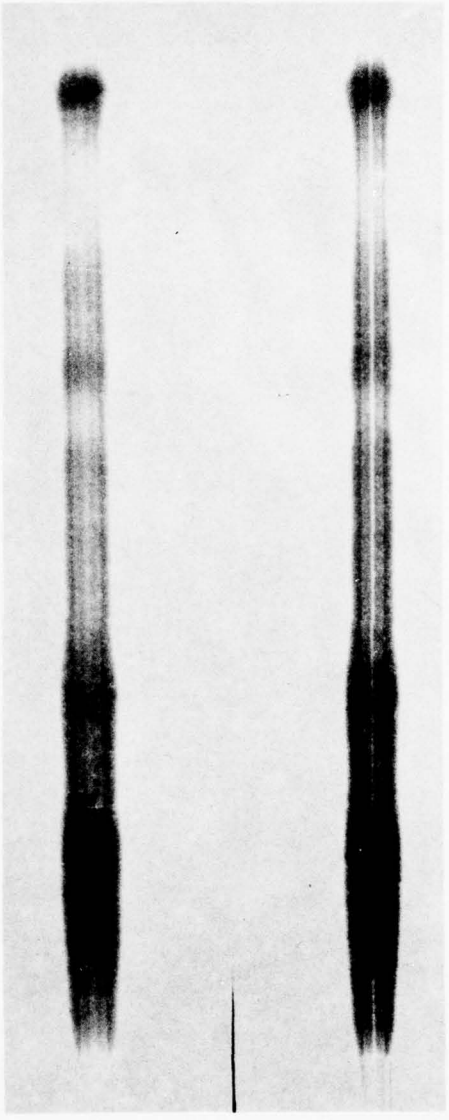

Sample No. 262

H V

PBN-77-67

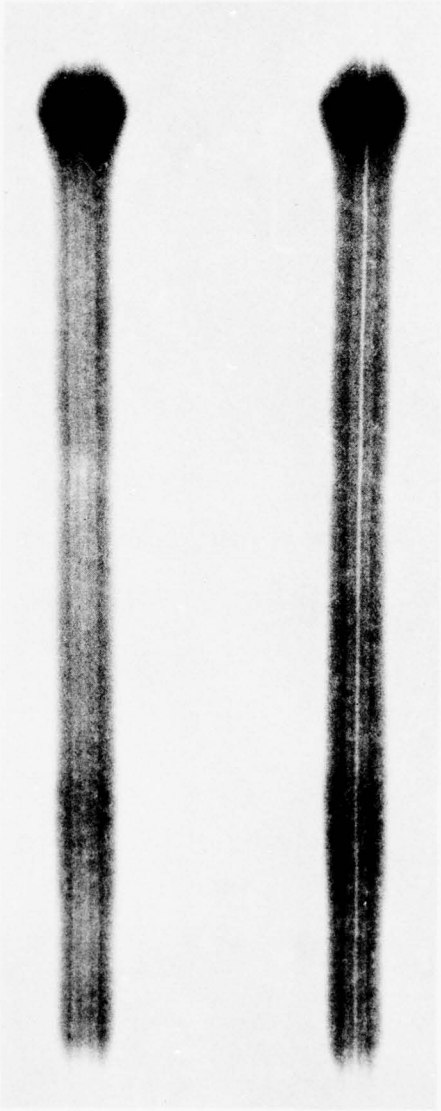

Sample No. 263

H V

PBN-77-68

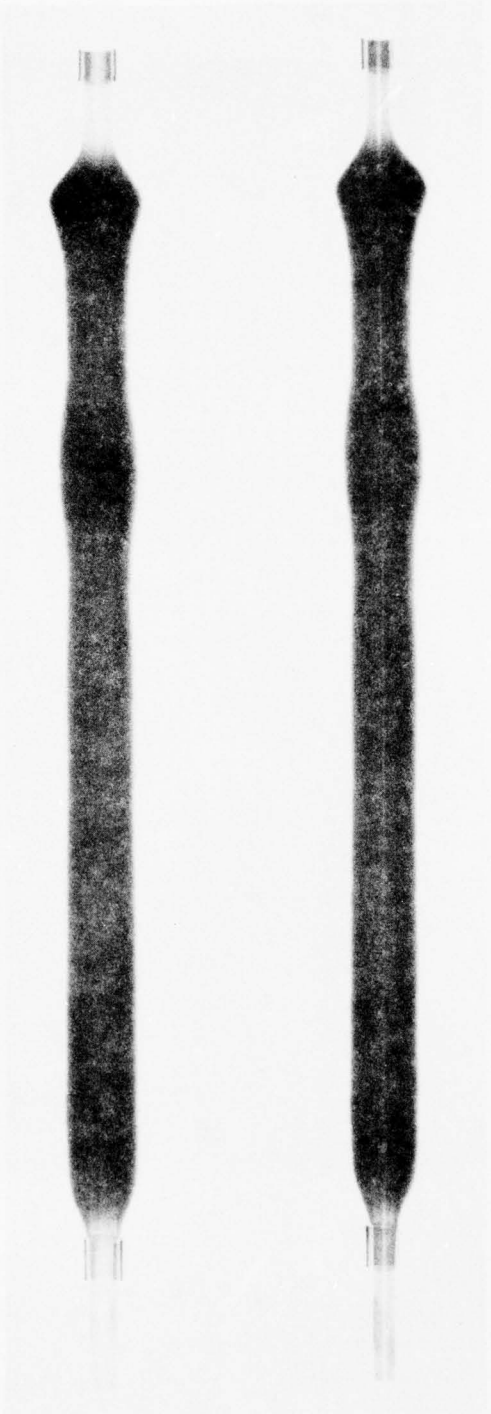

Sample No. 264

H V

PBN-77-69

Sample No. 266

H V

PBN-77-70

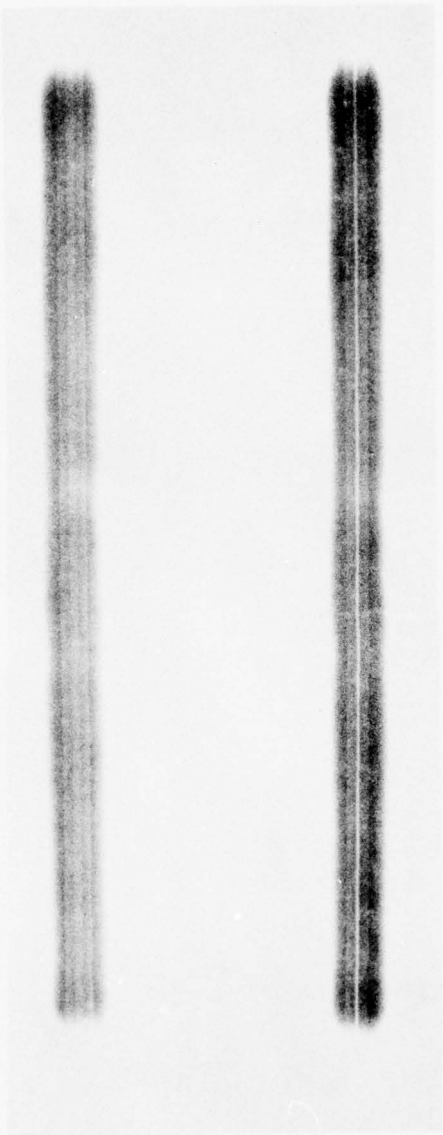

Sample No. 268

H V

PBN-77-71

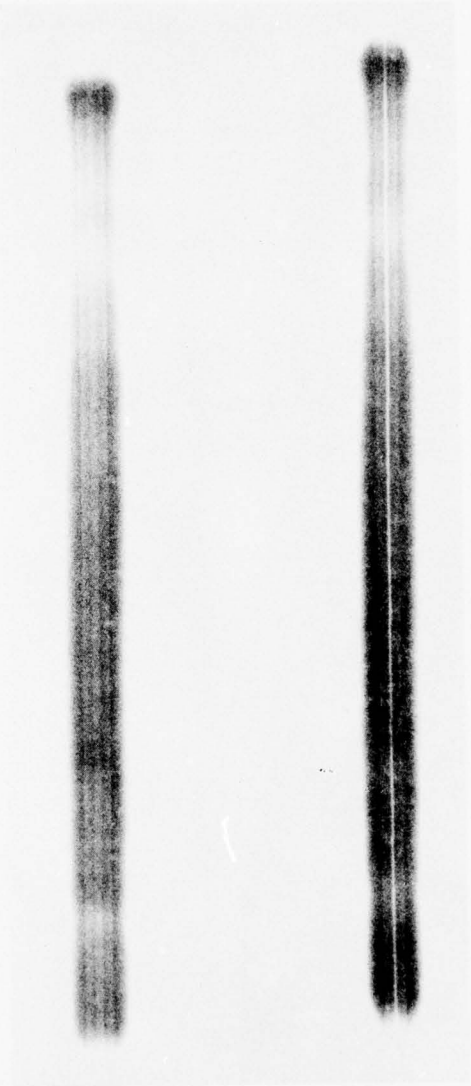

Sample No. 269

H V

PBN-77-72

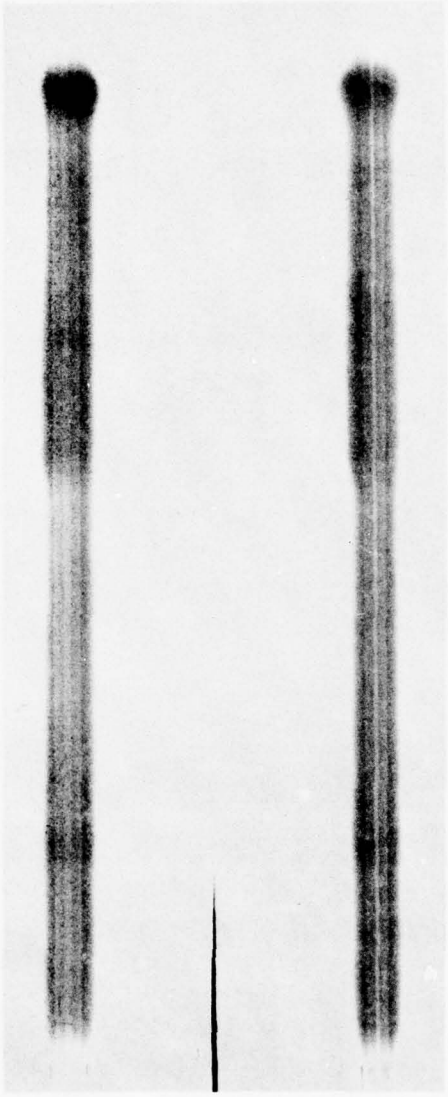

Sample No. 270

H V

PBN-77-73

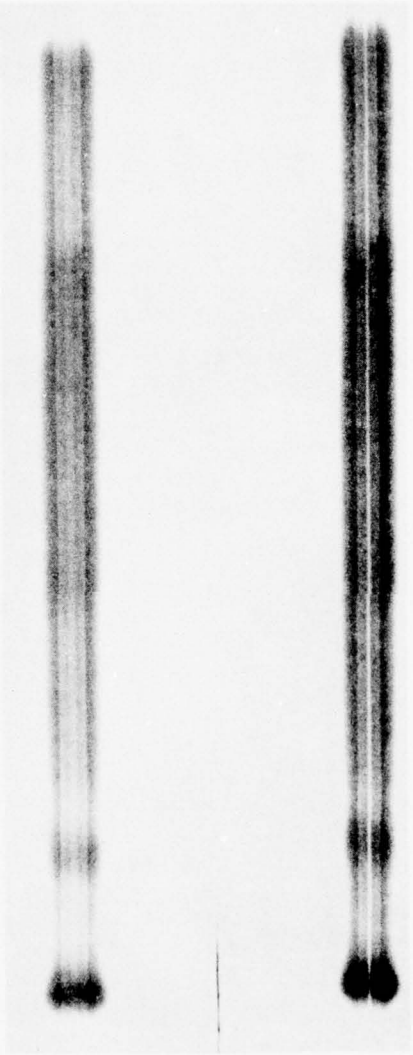

Sample No. 272

H V

PBN-77-74

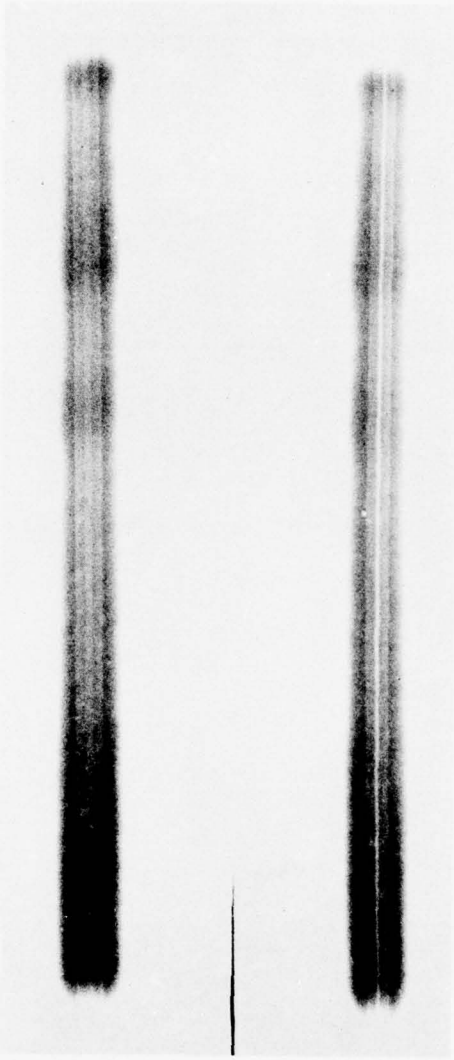

Sample No. 273

H V

PBN-77-75

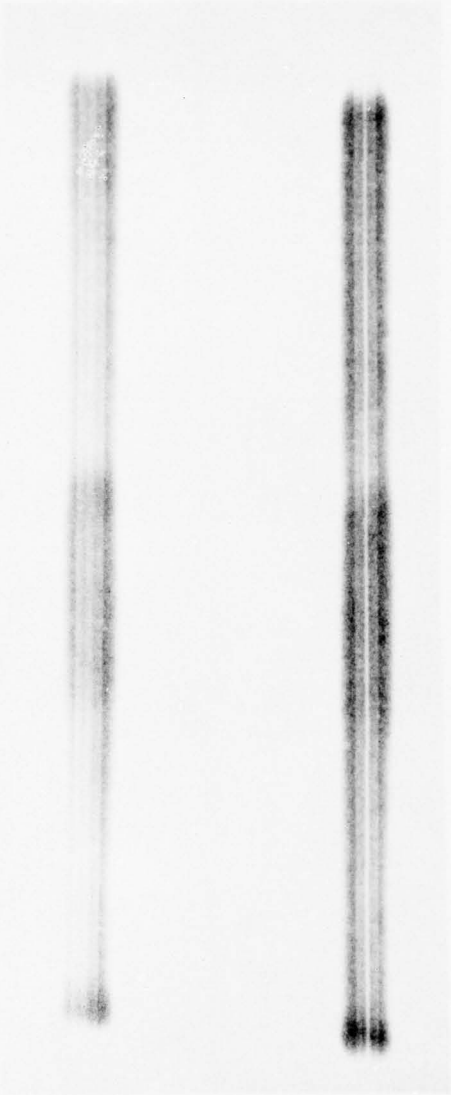

Sample No. 274

H V

PBN-77-76

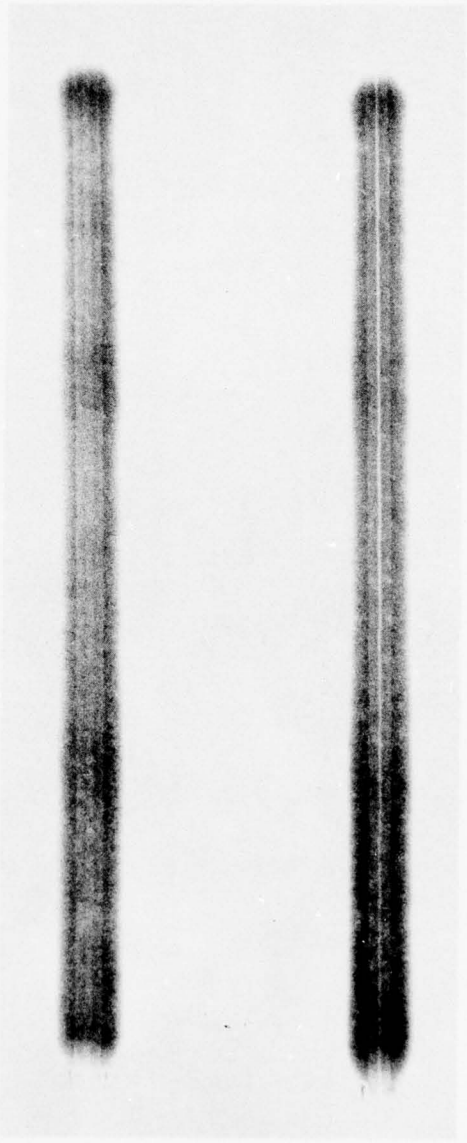

Sample No. 275

H V

PBN-77-77

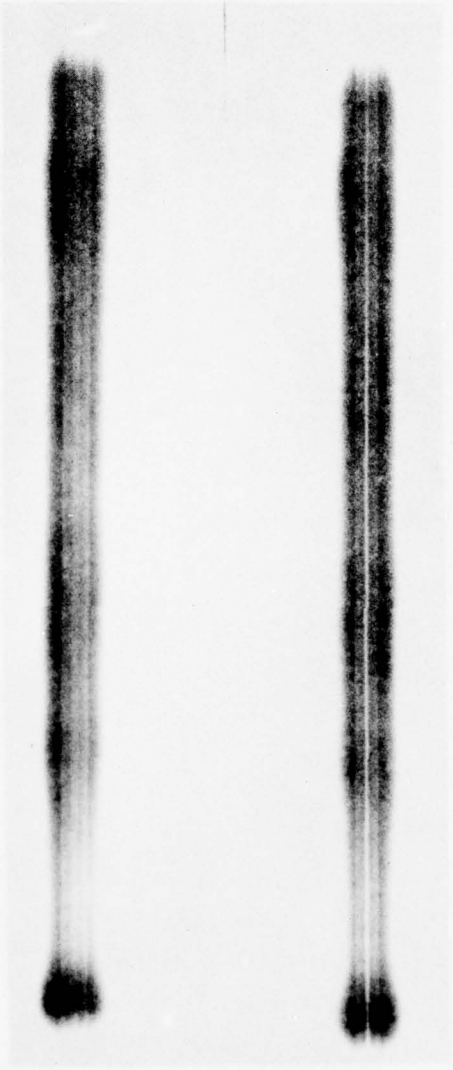

Sample No. 276

H V

PBN-77-78

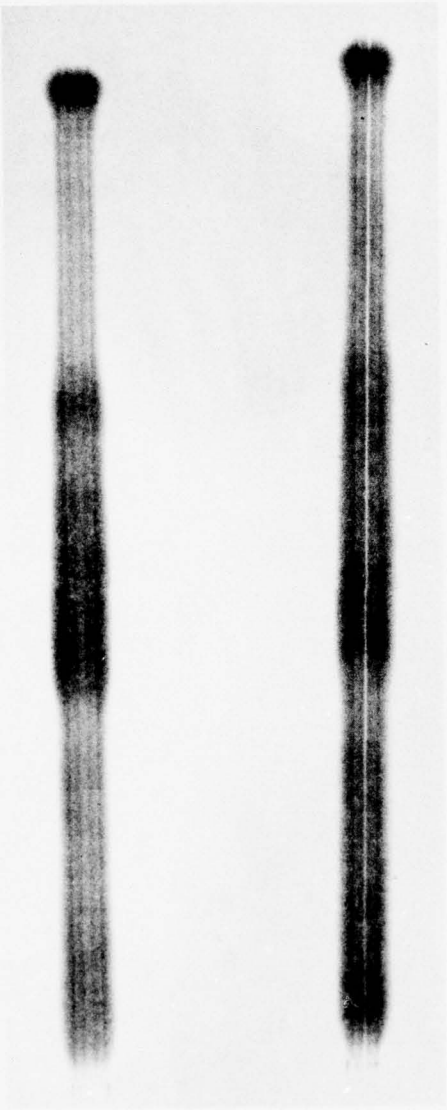

Sample No. 277

H V

PBN-77-79

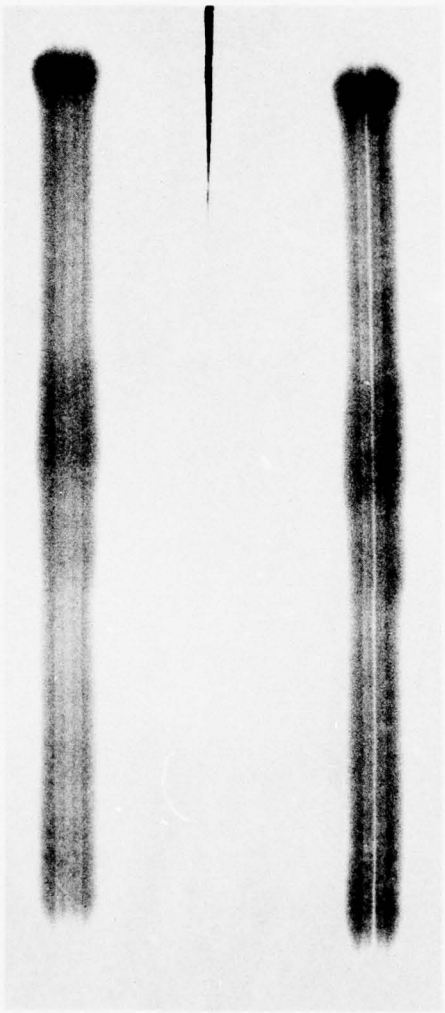

Sample No. 278

H V

PBN-77-80

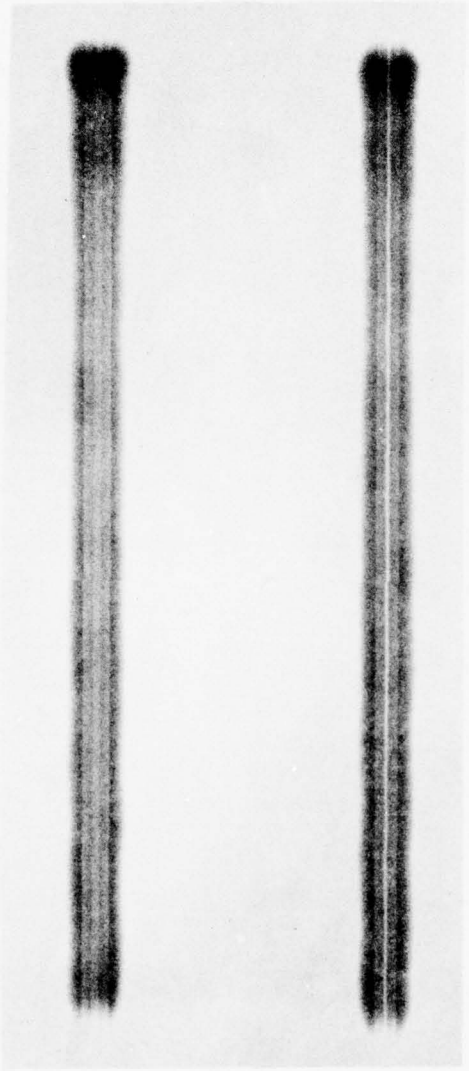

Sample No. 279

H V

PBN-77-81

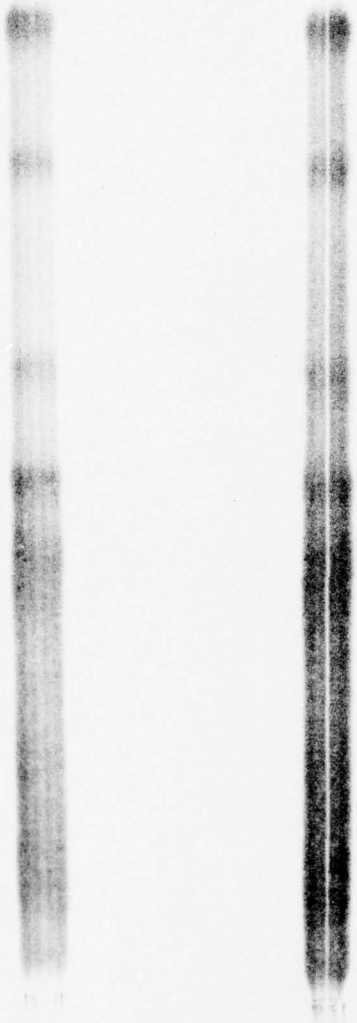

Sample No. 280

H V

PBN-77-82

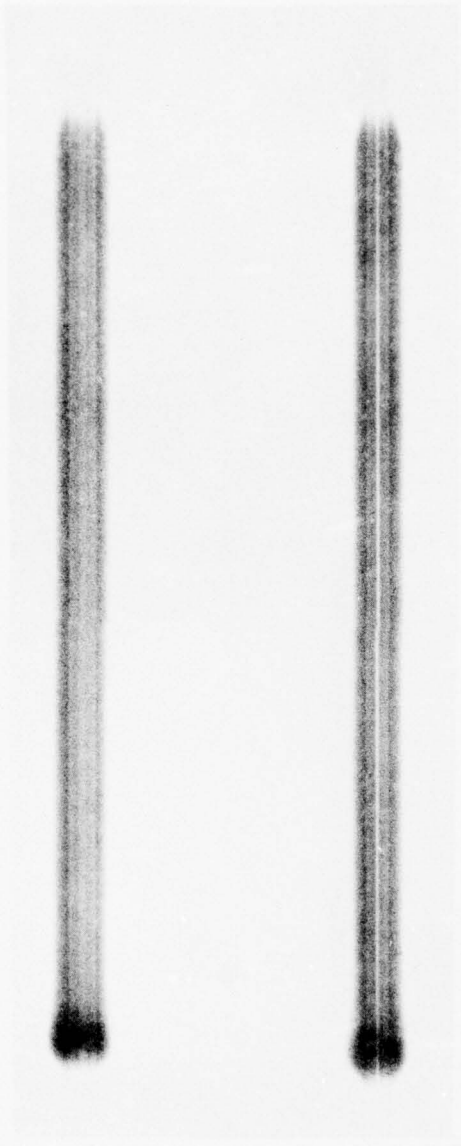

Sample No. 281

H V

PBN-77-83

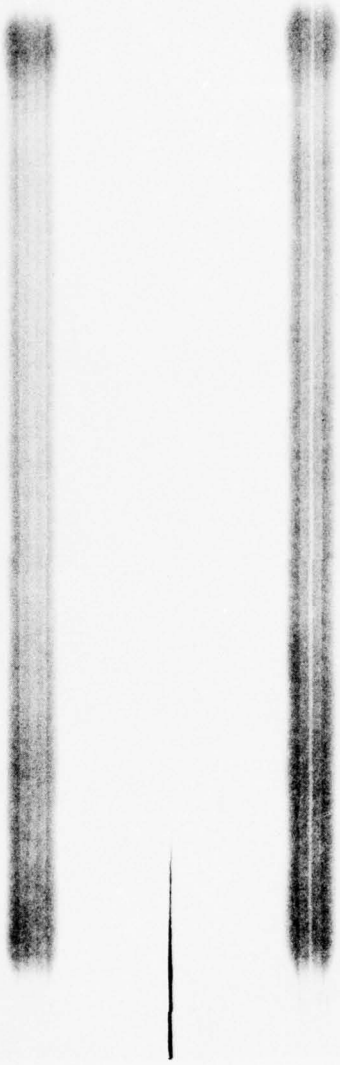

Sample No. 282

H V

PBN-77-84

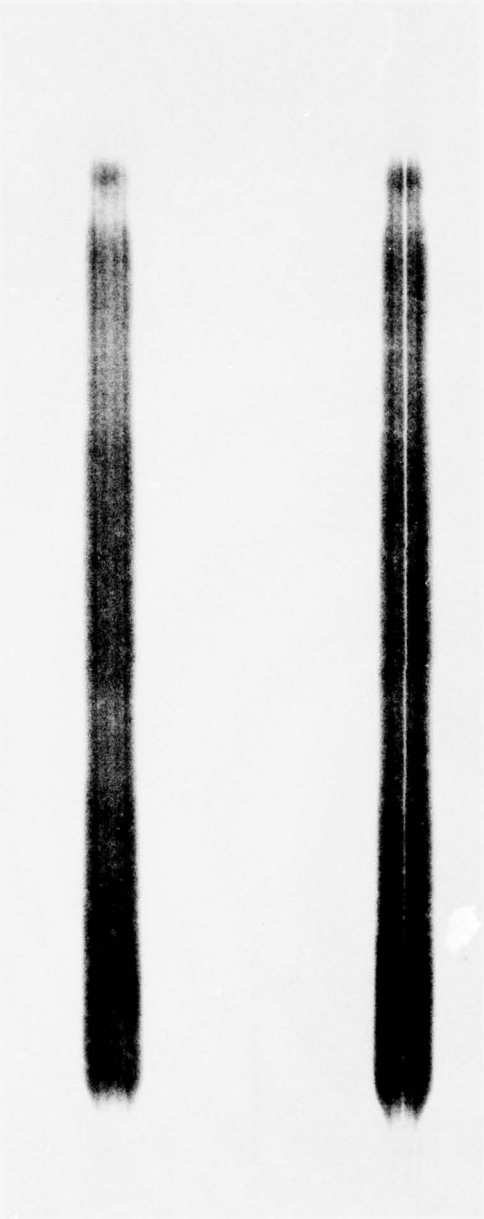

Sample No. 284

H V

PBN-77-85

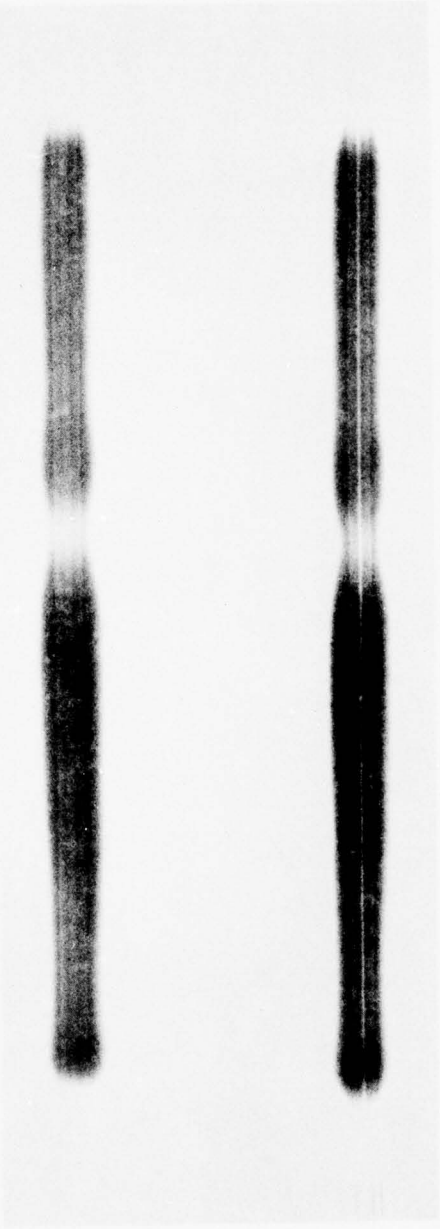

Sample No. 286

H V

PBN-77-86

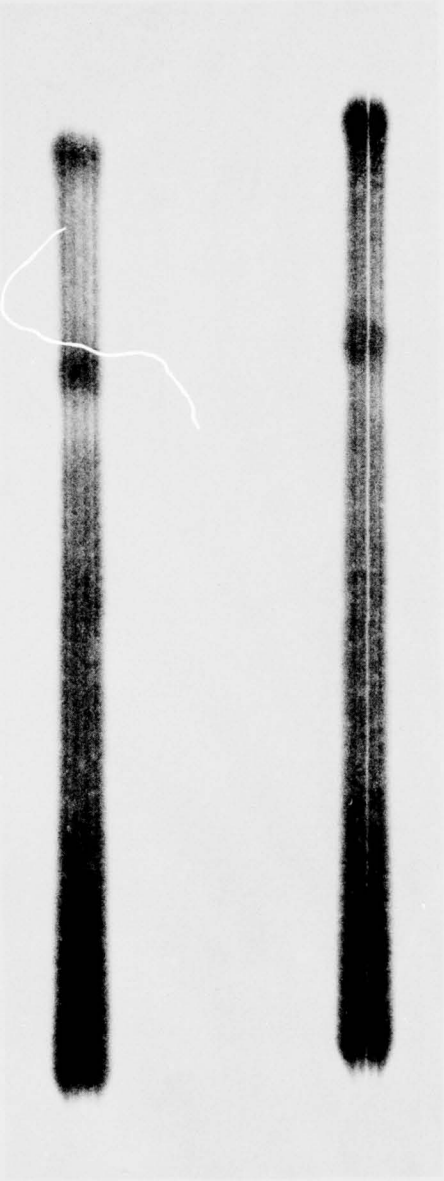

Sample No. 287

H V

PBN-77-87

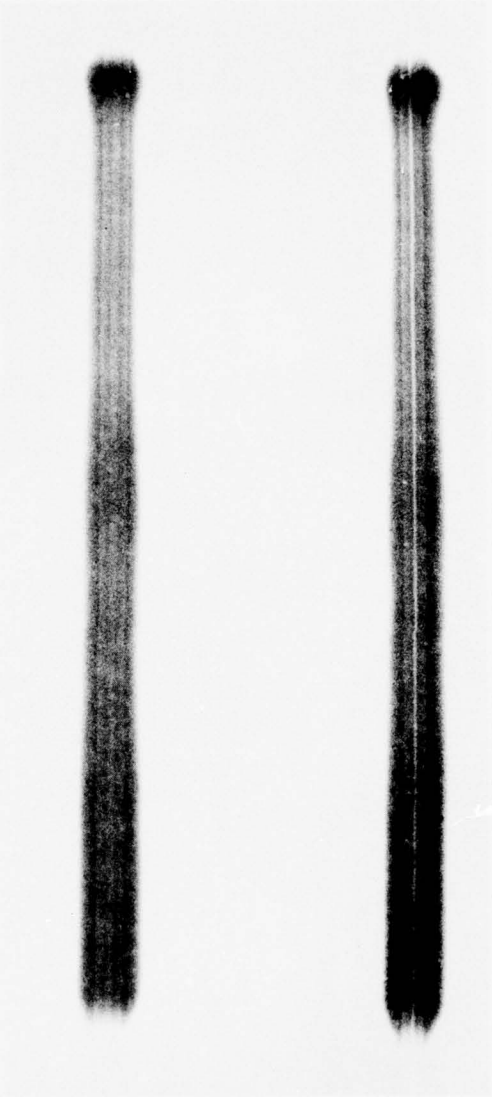

Sample No. 288

H V

PBN-77-88

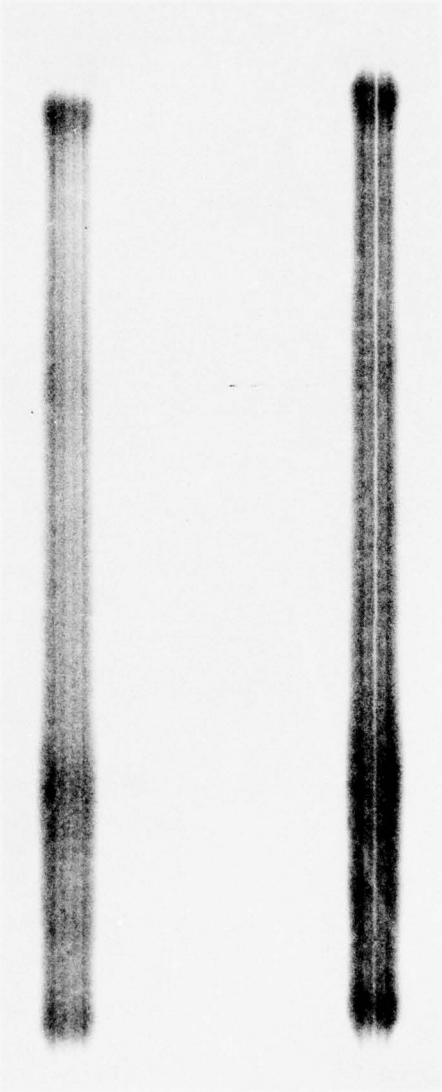

Sample No. 289

H V

PBN-77-89

Sample No. 290

H V

PBN-77-90

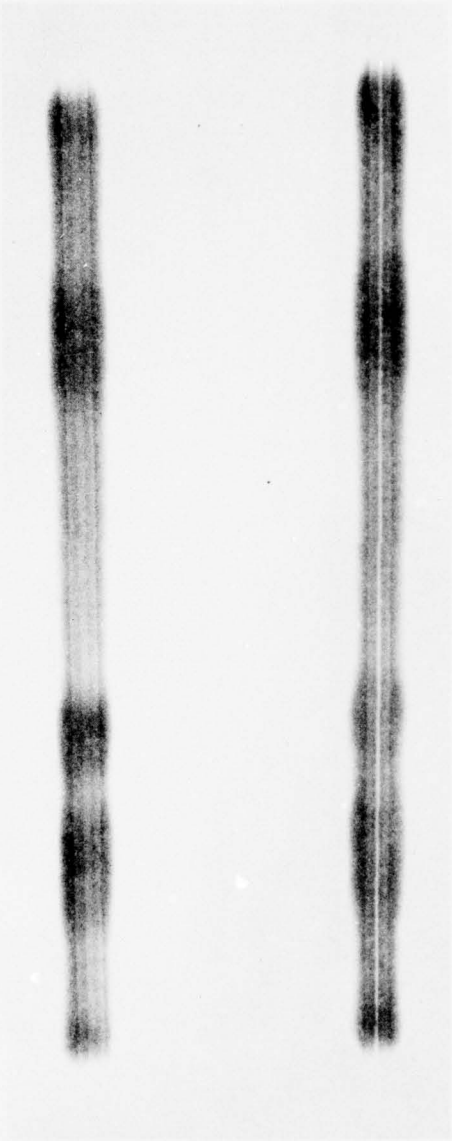

Sample No. 291

H V

PBN-77-91

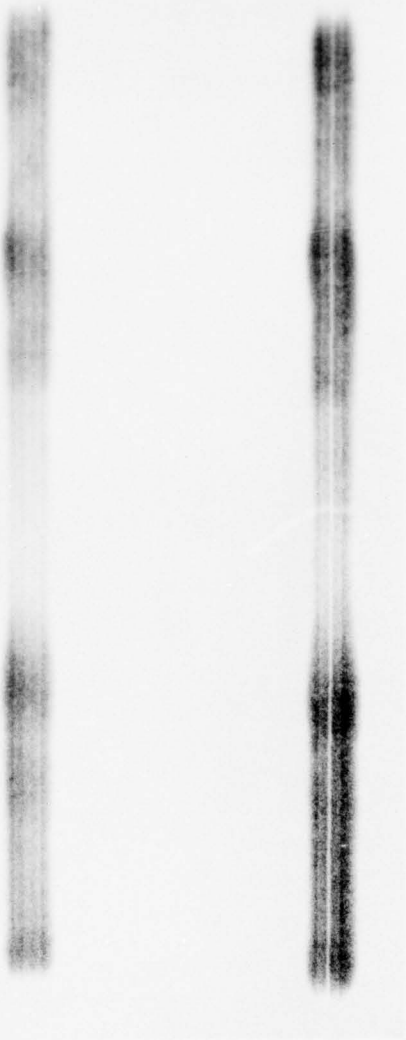

Sample No. 293

H V

PBN-77-92

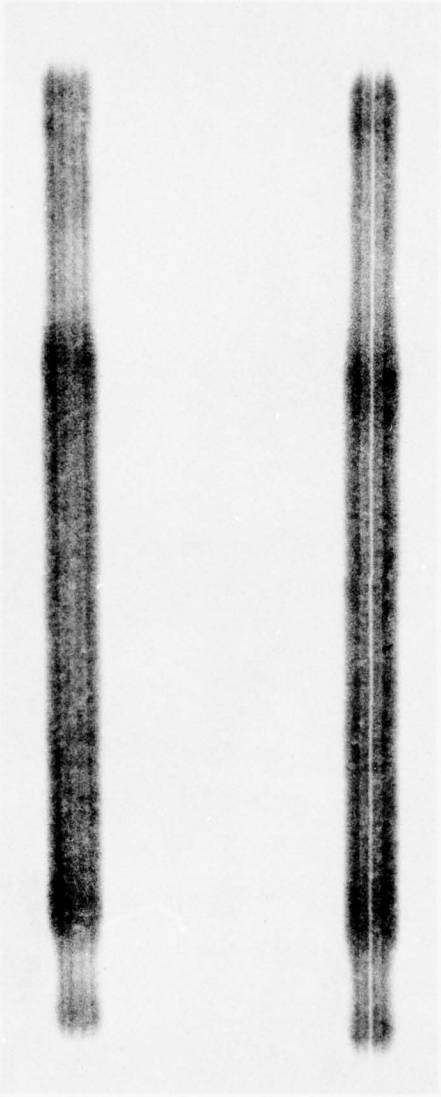

Sample No. 294

H V

PBN-77-93

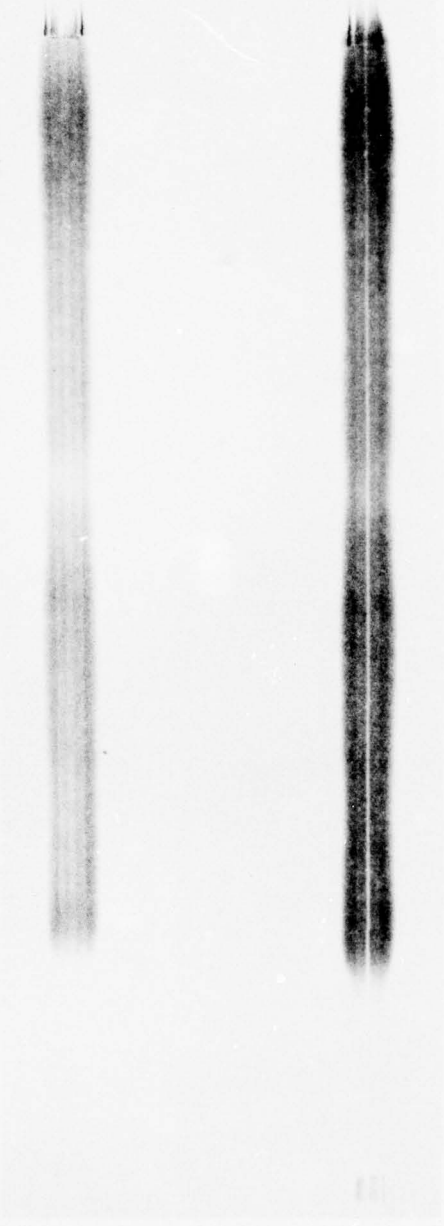

Sample No. 295

APPENDIX B

X-RADIOGRAPHY OF PHASE SHIFTERS 137-239

B.1 Introduction

We used a conventional x-ray fluoroscope (Radifluor 360, Torr X-ray Corp.) to take the transmission photographs of the phase-shifter elements in two orthogonal directions. Samples were placed directly on Kodak-type M film and irradiated at 80 KV 3 mA for 3-4 minutes with lead screen intensification. This produced full-size negatives with shades of gray, depending on transmitted intensity. The photographs shown on the data sheets are prints of these negatives in which the lighter areas indicate greater x-ray transmission.

Looking at the first (sample APS 137), the narrowest strip ~.005 in.) in the center region represents transmission by x-rays through the slot between the dielectric halves. At a greater distance from the center (~0.010 in. at either side) one observes the sides of the central wire slot. In this sample ferrite powder has blocked this slot, especially in the region between the arrows in both photographs. The next darker gray regions on either side of the centerline represents the dielectric material plus ferrite, and the outermost dark strips are the ferrite sidewalls as seen from the edge on. In the photograph on the right the join between dielectric halves lies in the plane of the paper and is therefore not seen. The center strip is the .040 in. wide dimension of the center slot, the darker group regions are dielectric, and the outermost strips are the ferrite top and bottom walls seen on edge. The darker areas in the center slot region indicate ferrite powder clogging the hole. This is the reason hysteresis data were not taken.

In the data tabulations on each sample sheet, the thickness of the thinnest ferrite wall is recorded at different positions and an average value is calculated. We have made the assumption that the value of B_r for uniform 50-mil walls all around would be 800 gauss (30 amp-turns) with the G-4 ferrite and 850 gauss (30 amp-turns) with the G-5 compositions. If the walls are nonuniform, the thinnest wall will be flux-limiting, and we assume it will cover the value of B_r by the percentage proportional to the departure from a uniform 50-mil wall. Other factors, such as longitudinal cracks or poor density ferrite, doubtless also have an effect on B_r. The simple correction based on percent cross-sectional reduction on the thin wall region, however, has been a rather effective explanation of reduced B_r. Its effectiveness is evident in a comparison of the estimated value with the measured value.

B.2 Discussion of Individual Samples

APS 137 had relatively uniform walls and probably would have been a good sample were it not for the powder clogging, indicated between the arrows.

APS 142 was only slightly bowed but broke in half (see arrow) during handling.

APS 143 had a thin wall, shown on the left side of the right-hand photograph. This was primarily a machining error.

APS 146 had some bow and a thin ferrite wall on the far left. The wall thickness at the ends again indicates a machining error.

APS 159 had a thin ferrite wall, again on the far left. Note that the broad dimension of the center slot was perpendicular to the join between dielectrics (see Fig. 1a), in contrast to previous samples.

APS 161 had the same slot orientation (wide dimension perpendicular to join) as APS 159. The walls were more nearly uniform than APS 159, and the measured B_r was ~100 gauss above the estimated value.

APS 162 was very similar to APS 161 in both appearance and B_r.

APS 164 was bowed in the weak direction (photograph on the right), where the curvature lay in the plane containing the thin (0.060 in.) dielectric dimension. It was equally bowed in the strong direction (0.150 in. dimension of the dielectric). This implies that the distorting forces were strong enough to bend the sample in directions dictated by spray conditions, independent of the cross-sectional geometry of the dielectric.

The ferrite wall on the far right was very thin (only 58 percent of the ideal thickness).

APS 169 showed bowing, primarily in the strong cross-sectional direction in the right-hand photograph.

APS 173 had a thin wall on the right side of the left-hand photograph. The separation of dielectric halves, especially toward the lower half, was particularly evident.

APS 179 showed one very thin wall on the far left, which was primarily a machining error, but also due to bowing in the weak direction.

APS 180 showed pronounced bowing in both orthogonal views and a thin wall on the far right.

APS 181 was given an extra-high temperature anneal, and developed some longitudinal cracks, which degraded B_r. Because longitudinal cracks generally lie in the plane of the dielectric join, this type is usually not shown by the radiographs.

APS 182 had a .010 in. bow in the strong direction and essentially none in the weak direction.

APS 183 had a bow B_r due partly to thin ferrite walls on the left side of the left photograph and right side of the right.

APS 184 had a very low B_r due to an extremely narrow wall on the far right.

APS 199 had a very low B_r due primarily to the low-temperature anneal, although wall uniformity was also poor.

APS 198 again had no anneal.

APS 202 had a thin ferrite wall on the far left and poor annealing condition.

APS 204 was subjected to the same anneal as APS 202 and shows low B_r.

APS 205 broke near one end during handling. The ferrite wall on the left side of the right photograph was as thin as .012 in.

APS 207 showed lens-shaped separations of the ferrite coating in the left photo, but strangely none on the right photograph.

APS 210 had a very thin wall due to bowing in the weak direction, as shown in the left photograph.

APS 211 was broken during handling. Other transverse cracks are seen throughout this sample.

APS 213 had a very narrow wall (as narrow as .010 in. in the weak direction).

APS 215 was broken during machining and was finished as a short phase shifter. No measurements were taken because of problems threading the wires.

APS 216 had broken during the process at two places (see arrows). Enhanced dielectric separation in these areas suggests that strain was relieved by cracking.

APS 217 was cracked halfway through, just as APS 216. Displacement of the crack edges (see arrow) again indicates release of internal stresses.

APS 219 was the second element sprayed with the G-5 powder.

APS 224 showed ferrite separation from the dielectric core and numerous transverse cracks.

APS 225 showed some bowing in both directions, but nevertheless was a satisfactory sample.

APS 227 showed bowing in the strong direction and separation between ferrite and dielectric throughout.

APS 231 was free of ferrite-dielectric separations but had nonuniform walls.

APS 234 showed very uniform walls and a high B_r.

APS 237 was similar to APS 234 but showed some bow in the weak direction (left photograph).

APS 238 showed good wall uniformity, but the separation of dielectric halves (left photo) was more than APS 234.

APS 239 showed some ferrite-dielectric separation (see arrow) and separation of insert halves, but the walls were reasonably uniform.

A. P. S. 137

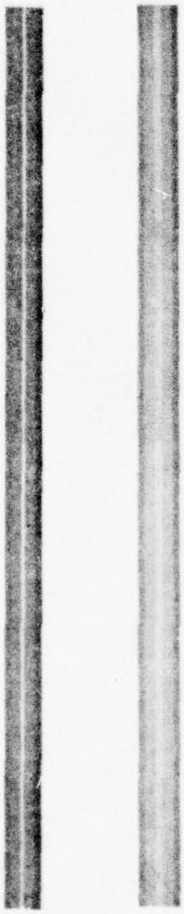

H_c = B_r = at ampere turns.

Anneal: 1010° 1.5 hrs. O_2

Distortions:

Bow: nil

Separation of insert halves: .004 in. full length

Wide-slot dimension: Parallel to join ☒

Perpendicular to join ☐

Thin-wall dimensions (mils):

End: 45
Center: 42
End: 42
Minimum: 42
Average: 43

Average thin-wall dimension as percentage of ideal .050": 86 percent.

Estimated B_r based on cross-section: B_r =

COMMENTS:

No hysteresis data, ferrite powder obstructing slot (see area between arrows) made th eading wires impossible. Ferrite coating too thin on one corner over full length. No cracks.

A. P. S. 142

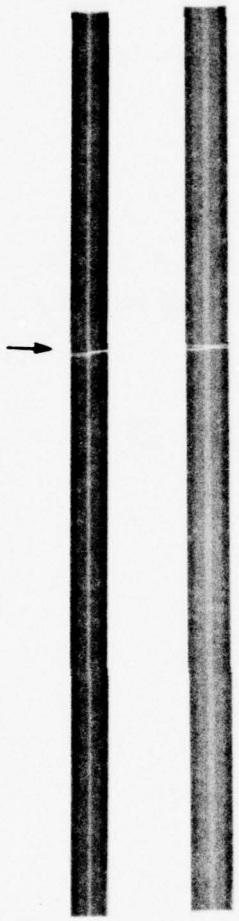

H_c = 2.50 B_r = 689 at 30 ampere turns.

Anneal: 1015° 2 hrs. O_2; 800° 2 hrs. O_2

Distortions:

Bow: .003 in.

Separation of insert halves: .003

Wide-slot dimension: Parallel to join ☒ Perpendicular to join ☐

Thin-wall dimensions (mils):

End: 40
Center: 43
End: 45
Minimum: 40
Average: 42.5

Average thin-wall dimension as percentage of ideal .050": 85 percent.

Estimated B_r based on cross-section: B_r = 680

COMMENTS:

Sample broke in half (see arrow). In weak direction machining was slightly skewed, thinner on left at top and on bottom right.

A. P. S. 143

H_c = 2.74 B_r = 626 at 30 ampere turns.

Anneal: 1010° 1.5 hrs. O_2; 800° 2 hrs. Air

Distortions:

Bow: .004 in.

Separation of insert halves: .006 in. for 2/3 length

Wide-slot dimension: Parallel to join ☒

Perpendicular to join ☐

Thin-wall dimensions (mils):

End: 37
Center: 36
End: 45
Minimum: 36
Average: 39

Average thin-wall dimension as percentage of ideal .050": 79 percent.

Estimated B_r based on cross-section: B_r = 629

COMMENTS:

Thin wall in strong direction due primarily to machining error.

A. P. S. 146

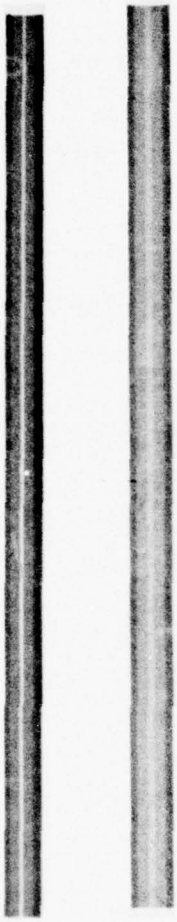

H_c = 2.73 B_r = 587 at 30 ampere turns.

Anneal: 1010° 1.5 hrs. O_2; 1000° 1 hr. Air

Distortions:

Bow: .005 in.

Separation of insert halves: .006 in.

Wide-slot dimension: Parallel to join ☒ Perpendicular to join ☐

Thin-wall dimensions (mils):

End: 45
Center: 35
End: 40
Minimum: 35
Average: 40

Average thin-wall dimension as percentage of ideal .050": 80 percent.

Estimated B_r based on cross-section: B_r = 640

COMMENTS:

Separation along most of the length. Thin wall primarily machining error.

A. P. S. 159

H_c = 2.46 B_r = 584 at 30 ampere turns.

Anneal: 1015° 1.5 hrs. O_2; 1050° 30 min. O_2

Distortions:

Bow:

Separation of insert halves: .007

Wide-slot dimension: Parallel to join ☐ Perpendicular to join ☒

Thin-wall dimensions (mils):

End: 40
Center: 25
End: 40
Minimum: 25
Average: 35

Average thin-wall dimension as percentage of ideal .050": 70 percent.

Estimated B_r based on cross-section: B_r = 560

COMMENTS:

Measured B_r before and after 1050°C anneal was unchanged.

A. P. S. 161

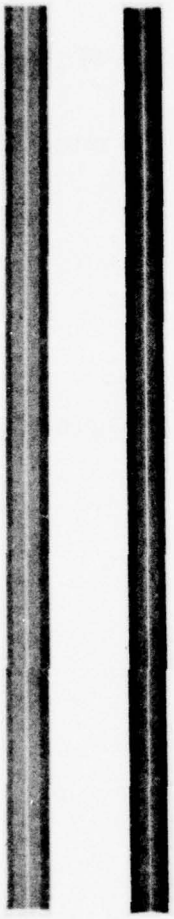

H_c = 3.37 B_r = 728 at 30 ampere turns.

Anneal: 1015° 1.5 hrs. O_2; 800° 10 hrs. Air

Distortions:

Bow: .005 in. weak dir.
Separation of insert halves: .005 in.

Wide-slot dimension: Parallel to join ☐
Perpendicular to join ☒

Thin-wall dimensions (mils):

End: 45
Center: 37
End: 40
Minimum: 37
Average: 41

Average thin-wall dimension as percentage of ideal .050": 81 percent.

Estimated B_r based on cross-section: B_r = 650

COMMENTS:

Measured B_r much higher than estimated value.

A. P. S. 162

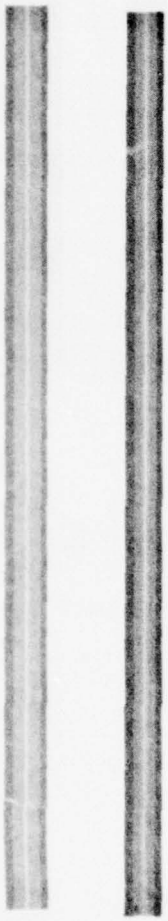

H_c = 3.19 B_r = 731 at 30 ampere turns.

Anneal: 1015° 1.5 hrs. O_2; 800° 10 hrs. Air

Distortions:

Bow: .005 in.

Separation of insert halves: .004 in.

Wide-slot dimension: Parallel to join ☐

Perpendicular to join ☒

Thin-wall dimensions (mils):

End: 40
Center: 37
End: 45
Minimum: 37
Average: 41

Average thin-wall dimension as percentage of ideal .050": 81 percent.

Estimated B_r based on cross-section: B_r = 651

COMMENTS:

Measured B_r much higher than estimated value. Probably represents a very dense sample.

PBN-77-112

A. P. S. 164

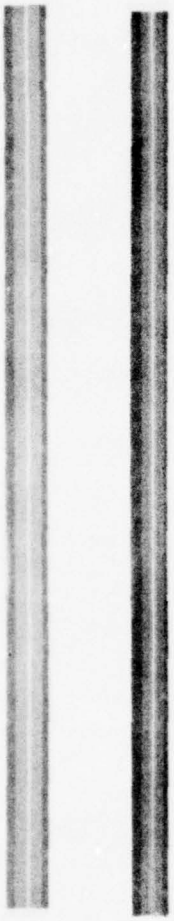

H_c = 2.75 B_r = 529 at 30 ampere turns.

Anneal: 1015° 1.5 hrs. O_2; 1050° 30 min. O_2;
800° 10 hrs. Air

Distortions:

Bow: .007 in. in weak direction, 005 in. in strong dir.

Separation of insert halves: .005 in.

Wide-slot dimension:

Parallel to join ☒

Perpendicular to join ☐

Thin-wall dimensions (mils):

End: 30
Center: 22
End: 35
Minimum: 20
Average: 29

Average thin-wall dimension as percentage of ideal .050": 58 percent.

Estimated B_r based on cross-section: B_r = 464

COMMENTS:

Sample warped in two directions. Thin wall partly due to machining error. Measured B_r much higher than calculated value, perhaps due to extra anneal.

A. P. S. 169

H_c = B_r = 664 at 30 ampere turns.

Anneal: 1015° 1.5 hrs. O_2; 800° 10 hrs. Air

Distortions:

Bow: .003 in.

Separation of insert halves: .004 in.

Wide-slot dimension: Parallel to join ☒ Perpendicular to join ☐

Thin-wall dimensions (mils):

End: 45
Center: 40
End: 45
Minimum: 40
Average: 43

Average thin-wall dimension as percentage of ideal .050": 86 percent.

Estimated B_r based on cross-section: B_r = 688

COMMENTS:

The substrate here is quite straight. The thin wall and low B_r is primarily grinding error.

A. P. S. 173

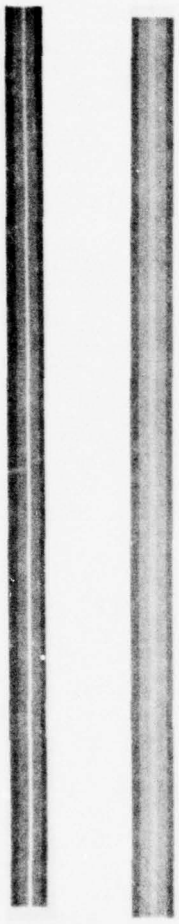

H_c = 3.41 B_r = 666 at 30 ampere turns.

Anneal: 1015° 1.5 hrs. O_2; 800° 2 hrs. Air

Distortions:

Bow: .020 in. in weak dir.
Separation of insert halves: .009 at one end

Wide-slot dimension: Parallel to join ☒
Perpendicular to join ☐

Thin-wall dimensions (mils):

End: 45
Center: 32
End: 35
Minimum: 30
Average: 37

Average thin-wall dimension as percentage of ideal .050": 74 percent.

Estimated B_r based on cross-section: B_r = 597

COMMENTS:

Wall thinness in weak direction at bottom end is due to separation of dielectric and poor machining rather than bowing.

A. P. S. 179

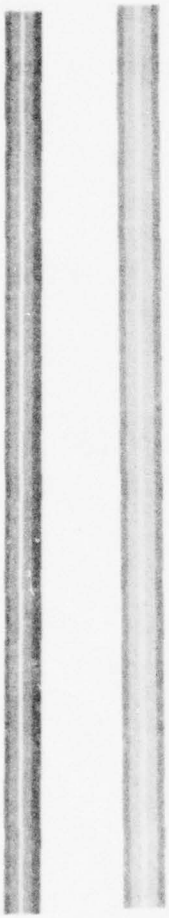

H_c = 3.45 B_r = 620 at 30 ampere turns.

Anneal: 1015° 1.5 hrs. O_2; 800° 2 hrs. Air

Distortions:

Bow: .005 in. in weak dir., 0 in strong dir.

Separation of insert halves: .007

Wide-slot dimension: Parallel to join ☒

Perpendicular to join ☐

Thin-wall dimensions (mils):

End: 40
Center: 35
End: 40
Minimum: 35
Average: 38

Average thin-wall dimension as percentage of ideal .050": 77 percent.

Estimated B_r based on cross-section: B_r = 613

COMMENTS:

Thin wall in weak direction appears to be primarily machining error.

A. P. S. 180

H_c = 3.28 B_r = 590 at 30 ampere turns.

Anneal: 1015° 1.5 hrs. O_2; 800° 10 hrs. Air

Distortions:

Bow: .010 in. in weak dir.; .015 in. in strong dir.

Separation of insert halves:

Wide-slot dimension: Parallel to join ☒ Perpendicular to join ☐

Thin-wall dimensions (mils):

End: 40
Center: 25
End: 45
Minimum: 25
Average: 37

Average thin-wall dimension as percentage of ideal .050": 73 percent.

Estimated B_r based on cross-section: B_r = 587

COMMENTS:

Bowing was major cause of thin wall in both weak and strong substrate directions.

A. P. S. 181

H_c = 2.82 B_r = 658 at 30 ampere turns.

Anneal: 1015° 1.5 hrs. O_2; 1016° 2 hrs. O_2

Distortions:

Bow: slight in both directions

Separation of insert halves: .005 in. to .002 in.

Wide-slot dimension: Parallel to join ☒

Perpendicular to join ☐

Thin-wall dimensions (mils):

End: 45
Center: 42
End: 45
Minimum: 42
Average: 44

Average thin-wall dimension as percentage of ideal .050": 88 percent.

Estimated B_r based on cross-section: B_r = 704

COMMENTS:

The extra high temperature anneal did not help because of extra cracking.

A. P. S. 182

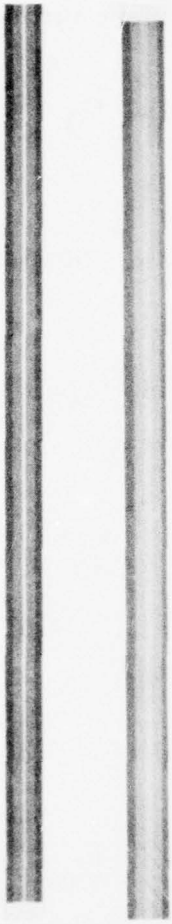

H_c = 3.18 B_r = 631 at 30 ampere turns.

Anneal: 1015° 1.5 hrs. O_2; 800° 2 hrs. Air

Distortions:

Bow: .010 in. in strong direction

Separation of insert halves: .004 in.

Wide-slot dimension: Parallel to join ☒

Perpendicular to join ☐

Thin-wall dimensions (mils):

End: 40
Center: 30
End: 40
Minimum: 30
Average: 37

Average thin-wall dimension as percentage of ideal .050": 73 percent.

Estimated B_r based on cross-section: B_r = 587

COMMENTS:

Agreement between measured and estimated B_r is good because cracks or other flaws such as insert separation are not observed. This shows that wall nonuniformities are the dominant contribution to the reduced B_r.

A. P. S. 183

H_c = 3.44 B_r = 607 at 30 ampere turns.

Anneal: 1015° 1.5 hrs. O_2; 800° 2 hrs. Air

Distortions:

Bow: .006 in. in strong dir.; zero in weak dir.

Separation of insert halves:

Wide-slot dimension: Parallel to join ☒

Perpendicular to join ☐

Thin-wall dimensions (mils):

End: 37
Center: 30
End: 35
Minimum: 27
Average: 34

Average thin-wall dimension as percentage of ideal .050": 68 percent.

Estimated B_r based on cross-section: B_r = 544

COMMENTS:

Thin wall due partly to poor machining and partly to bowing.

A. P. S. 184

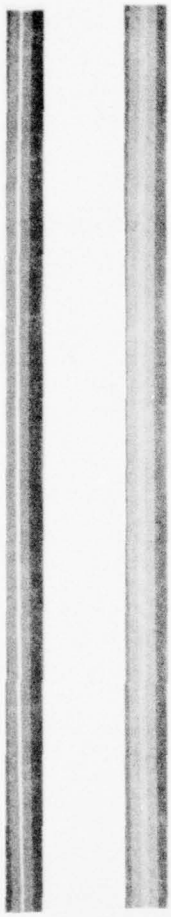

H_c = 3.40 B_r = 274 at 30 ampere turns.

Anneal: 1015° 1.5 hrs. O_2; 800° 2 hrs. Air

Distortions:

Bow: .027 in. in weak dir.; .020 in. in strong dir.

Separation of insert halves: .008 in.

Wide-slot dimension: Parallel to join ☒

Perpendicular to join ☐

Thin-wall dimensions (mils):

End: 22
Center: 3
End: 40
Minimum: 6
Average: 21

Average thin-wall dimension as percentage of ideal .050": 43 percent.

Estimated B_r based on cross-section: B_r = 346

COMMENTS:

This is probably the worst example of poor machining aggravated by warping in both strong and weak directions and separation of dielectric halves.

A. P. S. 197

H_c = 4.36 B_r = 366 at 30 ampere turns.

Anneal: 700° 6 hrs. Air

Distortions:

Bow: nil

Separation of insert halves: .005 in.

Wide-slot dimension: Parallel to join ☒

Perpendicular to join ☐

Thin-wall dimensions (mils):

End: 40
Center: 35
End: 32
Minimum: 32
Average: 36

Average thin-wall dimension as percentage of ideal .050": 71 percent.

Estimated B_r based on cross-section: B_r = 571

COMMENTS:

No high temperature anneal which was probably the major cause of low B_r.

PBN-77-122

A. P. S. 198

H_c = 3.24 B_r = 203 at 30 ampere turns.

Anneal: None

Distortions:

Bow: .005 in.

Separation of insert halves: .003 in. avg.

Wide-slot dimension: Parallel to join ☒

Perpendicular to join ☐

Thin-wall dimensions (mils):

End: 40
Center: 35
End: 40
Minimum: 35
Average: 38

Average thin-wall dimension as percentage of ideal .050": 76 percent.

Estimated B_r based on cross-section: B_r = 613

COMMENTS:

This sample had no anneal which resulted in the low B_r. Separation of dielectric is typical of most with minimal separation at the ends which are clamped during deposition.

A. P. S. 202

H_c = 2.39 B_r = 255 at 30 ampere turns.

Anneal: 1200° 30 min. O_2

Distortions:

Bow: .010 in. in weak dir.; .005 in. in strong dir.
Separation of insert halves: .003

Wide-slot dimension: Parallel to join ☒
Perpendicular to join ☐

Thin-wall dimensions (mils):

End: 35
Center: 27
End: 40
Minimum: 27
Average: 37

Average thin-wall dimension as percentage of ideal .050": 68 percent.

Estimated B_r based on cross-section: B_r = 544

COMMENTS:

Thin wall due to machining technique and to bowing. Excessive anneal temperature may have caused bowing.

A. P. S. 204

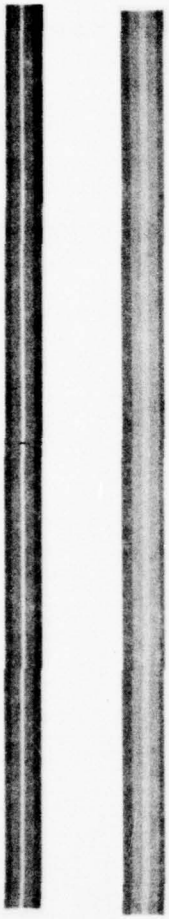

H_c = 2.60 B_r = 335 at 30 ampere turns.

Anneal: 1200° 30 min. O_2

Distortions:

Bow: .013 in. in weak dir.; .012 in. in strong dir.
Separation of insert halves: .005 in.

Wide-slot dimension: Parallel to join ☒
Perpendicular to join ☐

Thin-wall dimensions (mils):

End: 45
Center: 30
End: 40
Minimum: 30
Average: 38

Average thin-wall dimension as percentage of ideal .050": 76 percent.

Estimated B_r based on cross-section: B_r = 613

COMMENTS:

Low B_r is unexplained except by the excessive anneal temperature.

A. P. S. 205

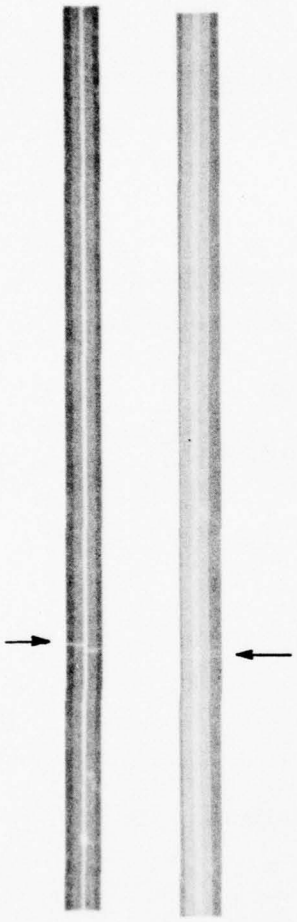

H_c = B_r = at ampere turns.

Anneal: 1200° 30 min. O_2

Distortions: .008 in.

Bow: .018 in. in strong direction; inch in weak dir.

Separation of insert halves:

Wide-slot dimension: Parallel to join ☒

Perpendicular to join ☐

Thin-wall dimensions (mils):

End: 37
Center: 15
End: 30
Minimum: 12
Average: 27

Average thin-wall dimension as percentage of ideal .050": 55 percent.

Estimated B_r based on cross-section: B_r = 437

COMMENTS:

Sample broke near one end (see arrows). Wall thinness due to poor machining and bow in strong direction. No hysteresis data.

A. P. S. 207

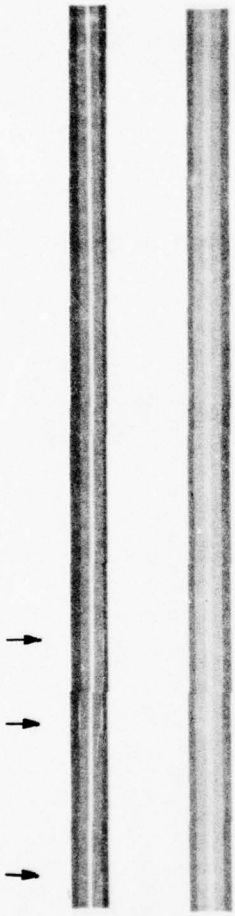

H_c = 2.57 B_r = 351 at 30 ampere turns.

Anneal: 1200° 30 min. O_2

Distortions:

Bow: .015 in. in weak dir.; nil in strong dir.

Separation of insert halves: .005 in. -.003 in.

Wide-slot dimension: Parallel to join ☒

Perpendicular to join ☐

Thin-wall dimensions (mils):

End: 45

Center: 20

End: 45

Minimum: 20

Average: 37

Average thin-wall dimension as percentage of ideal .050": 73 percent.

Estimated B_r based on cross-section: B_r = 587

COMMENTS:

Separation of ferrite coating at interface in weak direction (see arrows). Excessive anneal temperature.

A. P. S. 210

H_c = 2.71 B_r = 321 at 30 ampere turns.

Anneal: 1200° 30 min. O_2

Distortions:

Bow: .022 in. in weak dir.

Separation of insert halves: .005 in.

Wide-slot dimension: Parallel to join ☒

Perpendicular to join ☐

Thin-wall dimensions (mils):

End: 40
Center: 20
End: 45
Minimum: 20
Average: 35

Average thin-wall dimension as percentage of ideal .050": 70 percent.

Estimated B_r based on cross-section: B_r = 560

COMMENTS:

Bow in weak direction is extreme. Excessive anneal temperature.

PBN-77-128

A. P. S. 211

H_c = 2.81 B_r = 660 at 30 ampere turns.

Anneal: 1020° 2 hrs. O_2

Distortions:

Bow: .005 in. in weak dir.

Separation of insert halves: .003 in.

Wide-slot dimension: Parallel to join ☒

Perpendicular to join ☐

Thin-wall dimensions (mils):

End: 40

Center: 37

End. 45

Minimum: 35

Average: 41

Average thin-wall dimension as percentage of ideal .050": 81 percent.

Estimated B_r based on cross-section: B_r = 651

COMMENTS:

Sample broken during handling. Thin ferrite wall due primarily to machining error.

A. P. S. 213

H_c = B_r = at ampere turns.

Anneal: 1020° 2 hrs. O_2

Distortions:

Bow: .021 in. in weak direction.
Separation of insert halves: .008 in.

Wide-slot dimension: Parallel to join ☐
Perpendicular to join ☒

Thin-wall dimensions (mils):

End: 32
Center: 12
End: 35
Minimum: 10
Average: 26

Average thin-wall dimension as percentage of ideal .050": 53 percent.

Estimated B_r based on cross-section: B_r = 424

COMMENTS:

Extreme bow in weak direction. Also separation of dielectric halves worse than usual. One very thin wall in weak direction. No hysteresis data.

AD-A037 238 RAYTHEON CO WALTHAM MASS RESEARCH DIV F/G 9/5
MANUFACTURING METHODS AND TECHNOLOGY MEASURES FOR ARC-PLASMA-SP--ETC(U)
JAN 77 H J VAN HOOK, D MASSE, J SAUNDERS DAAB07-75-C-0043
UNCLASSIFIED S-2156 NL

2 OF 2
AD
A037238

END

DATE
FILMED
4-77

A. P. S. 215

H_c = B_r = at ampere turns.

Anneal: 1020° 2 hrs. O_2

Distortions:

Bow: .005 in. in weak dir.

Separation of insert halves: .005 in.

Wide-slot dimension: Parallel to join ☐

Perpendicular to join ☒

Thin-wall dimensions (mils):

End: 35

Center: 35

End: 45

Minimum: 35

Average: 38

Average thin-wall dimension as percentage of ideal .050": 77 percent.

Estimated B_r based on cross-section: B_r = 613

COMMENTS:

Extensive cracks through dielectric and ferrite. Short sample. No hysteresis data taken.

A. P. S. 216

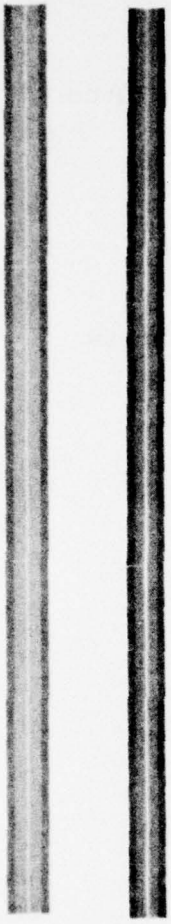

H_c = 2.76 B_r = 694 at 30 ampere turns.

Anneal: 1020° 2 hrs. O_2; 800° 2 hrs. Air

Distortions:

Bow:

Separation of insert halves: .010 in.

Wide-slot dimension: Parallel to join ☐ Perpendicular to join ☒

Thin-wall dimensions (mils):

End: 45
Center: 42
End: 45
Minimum:
Average: 44

Average thin-wall dimension as percentage of ideal .050": 88 percent.

Estimated B_r based on cross-section: B_r = 704

COMMENTS:

Cracks at 1/3 and 2/3 length (see arrows) extend through only one-half of element. Separations occur at these points. Cracks developed after machining because the surface is not straight.

A. P. S. 217

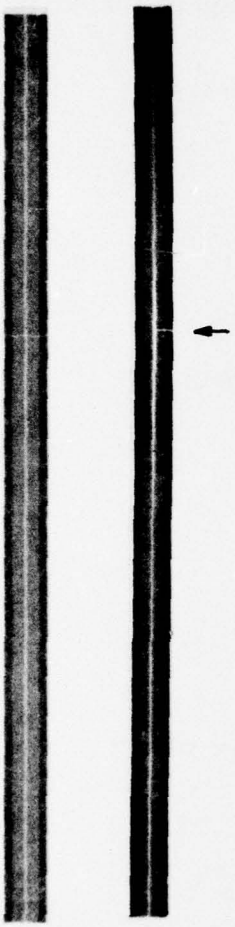

H_c = 2.71 B_r = 690 at 30 ampere turns.

Anneal: 1020° 2 hrs. O_2; 800° 2 hrs. Air

Distortions:

Bow: nil

Separation of insert halves: .020 in. at break

Wide-slot dimension: Parallel to join ☐

Perpendicular to join ☒

Thin-wall dimensions (mils):

End: 47
Center: 42
End: 42
Minimum: 42
Average: 44

Average thin-wall dimension as percentage of ideal .050": 87 percent.

Estimated B_r based on cross-section: B_r = 699

COMMENTS:

Element broken partially through after machining. Large separation of dielectric near break (see arrow).

A. P. S. 219

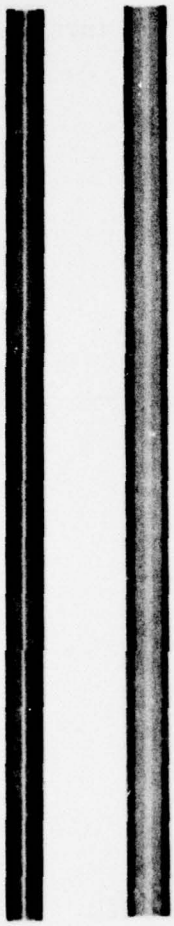

H_c = 3.89 B_r = 653 at 30 ampere turns.

Anneal: 1020° 2 hrs. O_2; 1016° 2 hrs. O_2

Distortions:

Bow: .005 in. in strong direction

Separation of insert halves: .005 in.

Wide-slot dimension: Parallel to join ☒

Perpendicular to join ☐

Thin-wall dimensions (mils):

End: 45

Center: 40

End: 45

Minimum: 40

Average: 43

Average thin-wall dimension as percentage of ideal .050": 87 percent.

Estimated B_r based on cross-section: B_r = 740
Assuming B_r = 850 gauss for uniform .050 in. walls

COMMENTS:

First use of the higher $4\pi M_s$ ferrite powder (LMTF475(G5)).

A. P. S. 224

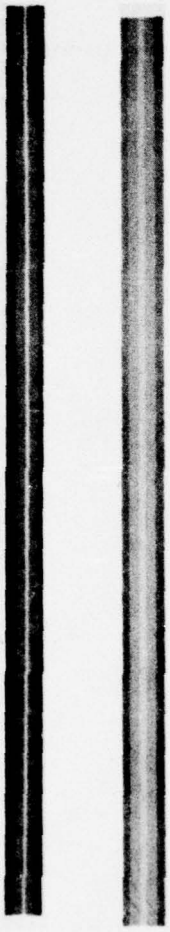

H_c = 2.76 B_r = 691 at 30 ampere turns.

Anneal: 1016° 3 hrs. O_2; 800° 2 hrs. Air

Distortions:

Bow: .021 in. in weak dir.

Separation of insert halves: .003 in.

Wide-slot dimension: Parallel to join ☒ Perpendicular to join ☐

Thin-wall dimensions (mils):

End: 47
Center: 30
End: 45
Minimum: 25
Average: 35

Average thin-wall dimension as percentage of ideal .050": 70 percent.

Estimated B_r based on cross-section: B_r = 560

COMMENTS:

Sample broken in handling. Separations between dielectric and ferrite coating in weak direction.

A. P. S. 225

H_c = 2.95 B_r = 758 at 30 ampere turns.

Anneal: 1016° 3 hrs. O_2; 800° 2 hrs. Air

Distortions:

Bow: .010 in. in weak dir.; .008 in. in strong dir.

Separation of insert halves:

Wide-slot dimension: Parallel to join [X]

Perpendicular to join [ ]

Thin-wall dimensions (mils):

End: 40
Center: 35
End: 45
Minimum: 32
Average: 40

Average thin-wall dimension as percentage of ideal .050": 80 percent.

Estimated B_r based on cross-section: B_r = 680

COMMENTS:

Used G-5 powder. Machining error as well as bowing contributed to wall nonuniformity.

A. P. S. 227

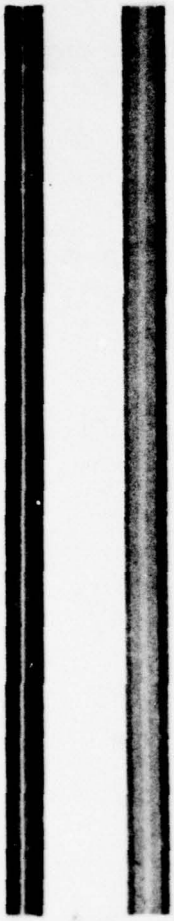

H_c = 2.0 B_r = 447 at 30 ampere turns.

Anneal: 1000° 5 hrs. O_2; 800° 2 hrs. Air

Distortions:

Bow: In strong direction

Separation of insert halves: 0 to .007, 004 in. avg.

Wide-slot dimension: Parallel to join ☒ Perpendicular to join ☐

Thin-wall dimensions (mils):

End: 35
Center: 25
End: 45
Minimum: 25
Average: 35

Average thin-wall dimension as percentage of ideal .050": 70 percent.

Estimated B_r based on cross-section: B_r = 595

COMMENTS:

Sample bowed in two directions. Separation of ferrite coating and abundant cracks in the dielectric. Used G5 powder.

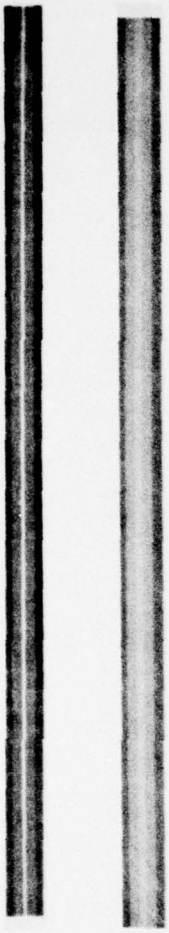

A. P. S. 231

H_c = 3.40 B_r = 664 at 30 ampere turns.

Anneal: 1000° 5 hrs. O_2; 800° 2 hrs. Air

Distortions:

Bow:

Separation of insert halves:

Wide-slot dimension: Parallel to join ☒

Perpendicular to join ☐

Thin-wall dimensions (mils):

End: 45
Center: 35
End: 42
Minimum: 35
Average: 41

Average thin-wall dimension as percentage of ideal .050": 81 percent.

Estimated B_r based on cross-section: B_r = 689

COMMENTS:

Bowed in both directions. Used G5 powder.

A. P. S. 234

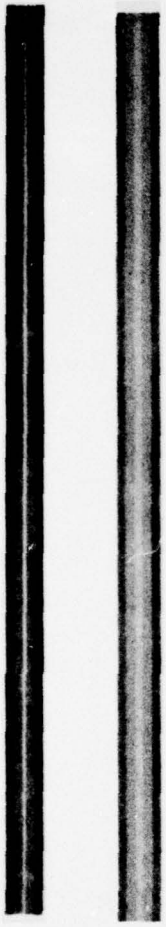

H_c = 3.12 B_r = 828 at 30 ampere turns.

Anneal: 1000° 5hrs. O_2; 800° 2 hrs. Air

Distortions:

Bow: nil

Separation of insert halves: nil

Wide-slot dimension: Parallel to join ☒

Perpendicular to join ☐

Thin-wall dimensions (mils):

End: 47

Center: 45

End: 50

Minimum:

Average: 47

Average thin-wall dimension as percentage of ideal .050": 95 percent.

Estimated B_r based on cross-section: B_r = 808

COMMENTS:

Best sample produced to date. Used the G5 ferrite powder.

A. P. S. 237

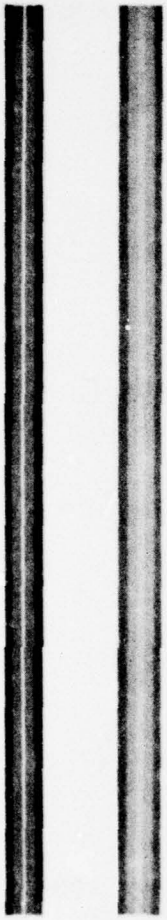

H_c = 3.11 B_r = 705 at 30 ampere turns.

Anneal: 1000° 2 hrs. O_2; 1015° 2 hrs. O_2;
800° 2 hrs. Air

Distortions:

Bow: .012 in. in weak dir.

Separation of insert halves: .005 in.

Wide-slot dimension: Parallel to join ☒
Perpendicular to join ☐

Thin-wall dimensions (mils):

End: 50
Center: 35
End: 45
Minimum: 35
Average: 43

Average thin-wall dimension as percentage of ideal .050": 87 percent.

Estimated B_r based on cross-section: B_r = 740

COMMENTS:

G-5 powder. No transverse cracks visible. This sample should give higher B_r, perhaps with longer anneal.

A. P. S. 238

H_c = 3.22 B_r = 740 at 30 ampere turns.

Anneal: 1000° 5 hrs. O_2; 1016° 2 hrs. O_2;
800° 2 hrs. Air

Distortions:

Bow: nil

Separation of insert halves: .007 in.

Wide-slot dimension: Parallel to join ☒

Perpendicular to join ☐

Thin-wall dimensions (mils):

End: 45

Center: 40

End: 42

Minimum: 40

Average: 42

Average thin-wall dimension as percentage of ideal .050": 85 percent.

Estimated B_r based on cross-section: B_r = 720

COMMENTS:

G5 powder. Sample free of transverse cracks. Separation of dielectric larger than usual.

A. P. S. 239

H_c = 2.93 B_r = 497 at 30 ampere turns.

Anneal: 1000° 5 hrs. O_2; 1016° 2 hrs. O_2;
800° 2 hrs. Air

Distortions:

Bow: .006 in. in strong dir.; .010 in. in weak dir.

Separation of insert halves: .005 in.

Wide-slot dimension: Parallel to join ☒
Perpendicular to join ☒

Thin-wall dimensions (mils):

End: 47
Center: 35
End: 40
Minimum: 37
Average: 41

Average thin-wall dimension as percentage of ideal .050": 81 percent.

Estimated B_r based on cross-section: B_r = 689

COMMENTS:

G5 powder. Bad separation of ferrite in weak direction (see arrow). Bowed in both directions.

DISTRIBUTION LIST

The Institute for Defense Analysis
Science and Technology Division
ATTN: Dr. Alvin D. Schnitzler
400 Army-Navy Drive
Arlington, VA 22202

Commander (2)
US Army Electronics Command
ATTN: DRSEL-PP-I-PI-1
(Mr. W. Peltz)
Fort Monmouth, NJ 07703

Dr. Joseph E. Rowe
Vice Provost and Dean
School of Engineering
Case Western Reserve University
312 Glennan Bldg.
Cleveland, OH 44106

Director, Applied Physics Laboratory
Sperry Research Center
ATTN: Dr. Richard Damon
Sudbury, MA 01776

Dr. Daniel G. Dow, Chairman
Dept. of Electrical Engineering
University of Washington
Seattle, Washington 98195

Commanding General
US Army Electronics Command
ATTN: DRSEL-TL-BM
(Mr. N.M. Wilson)
Fort Monmouth, NJ 07703

Commander
Harry Diamond Labs.
ATTN: AMXDO-RAA
(Mr.H.W.A. Gerlach)
2800 Powder Mill Road
Adelphi, MD 207833

Naval Electronics Laboratory Ctr
ATTN: Mr. E.D. Maynard, Jr.
Code 220
271 Catalina Blvd.
San Diego, CA 92152

Commander, RADC
Surveillance Technology Branch
ATTN: Mr. H. Chiosa, OCTE
Griffiss AFB, NY 13441

Director, National Security Agency
ATTN: Mr. A.T.Andrews, Jr. R335
Fort George G. Meade, MD 20755

Commander
US Army Production Equipment Agency
ATTN: AMXPE-MT (Mr. C.E. McBurney)
Rock Island, IL 61201

Advisory Group on Electron Devices (2)
ATTN: Working Group on Special
Devices
201 Varick Street
New York, NY 10014

Raytheon Company
Microwave and Power Tube Division
ATTN: L.L. Clampitt
190 Willow Street
Waltham, MA 02154

Dr. Turner E. Hasty, Director
Semiconductor, Research and Engr. Labs.
Texas Instruments, Inc.
PO Box 5013, M.S. 72
Dallas, TX 75222

Microwave Associates
ATTN: Dr. Joseph A. Saloom
Burlington, MA 01803

Commanding General
US Army Electronics Command
ATTN: DRSEL-TL-IM
(Mr. V.G.Gelnovatch)
Fort Monmouth, NJ 07703

US Army Ballistic Research Labs.
ATTN: Mr. D.G. Bauerle, AMXBR-CA
Aberdeen Proving Group, MD 21005

Director, US Army Ballistic Missile
Defense Advanced Technology Ctr.
ATTN: ATC-R, Dr. Bob L. Smith
P.O. Box 1500
Huntsville, AL 35807

Department of the Navy
US Naval Research Lab
ATTN: Mr. L. Whicker, Code 5250
Washington, DC 20390

Commander, AFAL
ATTN: AFAL/TE, Mr. J. Edwards
Wright-Patterson AFB, OH 45433

Lincoln Lab., MIT
ATTN: Dr. G.L. Guernsey
PO Box 73
Lexington, MA 02173

DISTRIBUTION LIST (CONTINUED)

AMPEX Corporation
ATTN: Mr. Gil Argentina 3-22
401 Broadway
Redwood City, CA 94063

US Army Missile Command
Directorate for Res. Engr. and
Missile Systems Lab.
ATTN: AMSMI-RLM
(Mr. P. Ormsby)
Redstone Arsenal, AL 35809

Microwave Applications Group
ATTN: Dr. Charles Boyd, Jr.
10021 Canaga Ave.
Chatsworth, CA 91311

US Army Elect Tech and Devices Lab(5)
ATTN: DRSEL-TL-MA
(Mr. Richard Babbitt)
Fort Monmouth, NJ 07703

NASA Headquarters
ATTN: Mr. C. E. Catoe
Code RES
Washington, D.C. 20546

Trans Tech, Inc.
ATTN: Mr. R. West
12 Meem Ave.
Gaithersburg, MA 20760

U.S. Army Missile Command
Director for Res. Engr. and Missile
Systems Lab.
ATTN: AMSMI-REI
(Mr. B. Spalding)
Redstone Arsenal, AL 35809

US Army Combat Surv and Target
Acq. Lab
ATTN: DRSEL-CT-R
Fort Monmouth, NJ 07703

Defense Documentation Center (12)
ATTN: DDC-IRS
Cameron Station (Bldg. 5)
Alexandria, VA 22314

Commander
US Army Electronics Command
ATTN: DRSEL-RD-ET-2
(Mr. Phillip Meltesen)
Fort Monmouth, NJ 07703